Chemoenzymatic synthesis of Tamsulosin.

Enol de Prado, Juan Mangas-Sánchez,* and Vicente Gotor-Fernández*

Organic and Inorganic Chemistry Department, Instituto Universitario de Química Organometálica "Enrique Moles", University of Oviedo. Avenida Julián Clavería 8, 33006 Oviedo, Asturias (Spain).
Telephone numbers: +34 985102982 (J.M.-S.) and +34 985103454 (V.G.-F.)
e-mail addresses: mangasjuan@uniovi.es (J.M.-S.) vicgotfer@uniovi.es (V.G.-F.)

SUPPORTING INFORMATION

Index (Page 1 out of 44)

I. Compounds described in this contribution

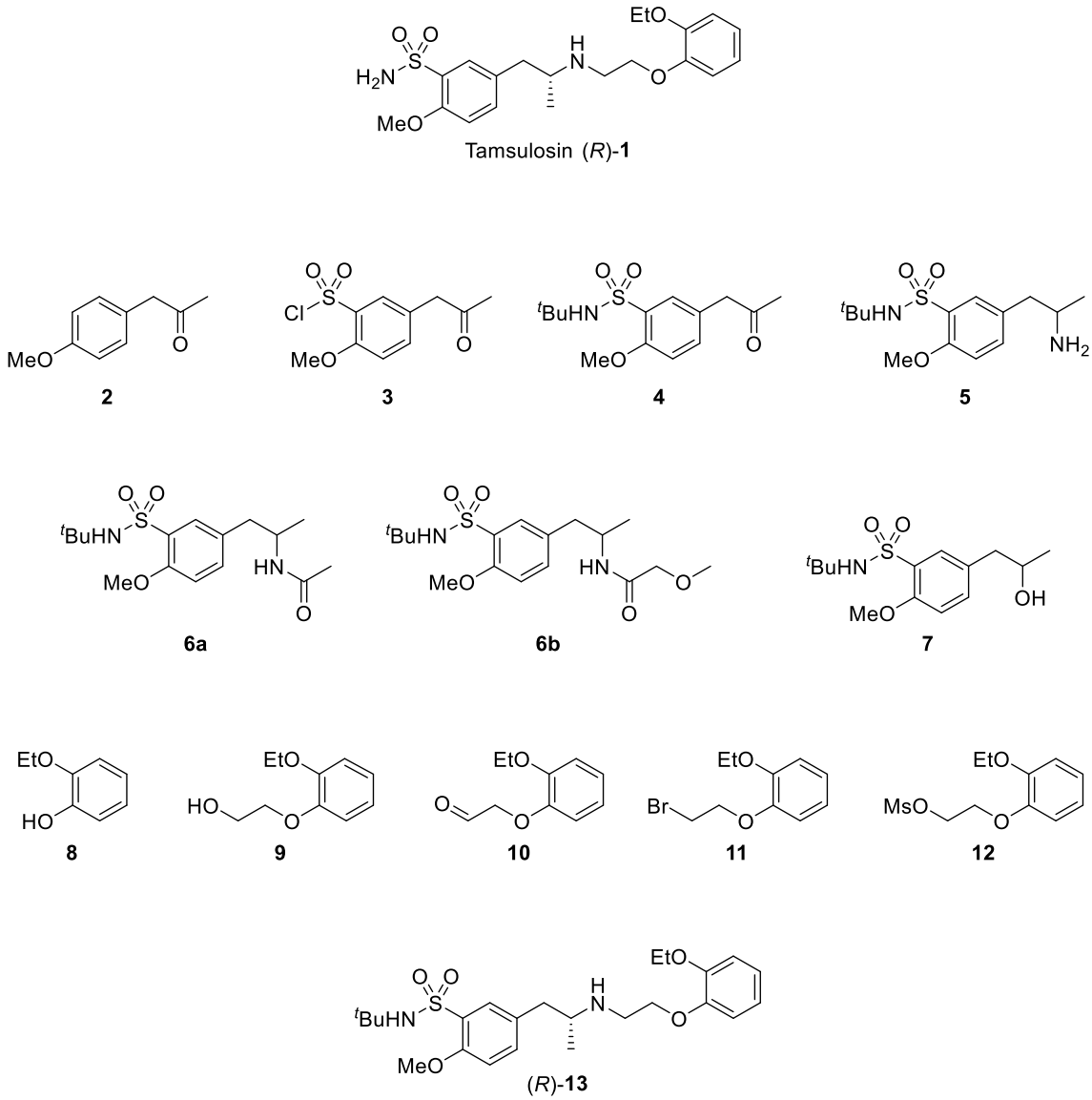

Figure S1. Compounds described in this contribution.

II. Biotransamination experiments

Table S1. Biotransamination of ketone **4** (25 mM) using 2-$PrNH_2$ (50 equiv) in KPi buffer (100 mM, pH 7.5) with 2-MeTHF as a cosolvent (2.5% v/v) after 24 h at 30 °C and 250 rpm.

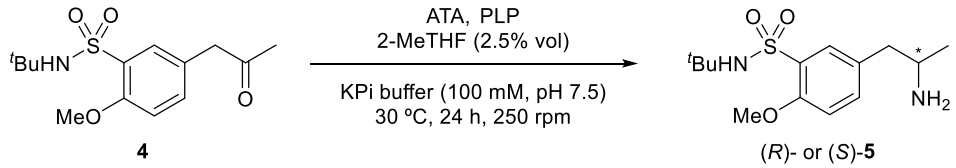

4 (*R*)- or (*S*)-**5**

Entry	ATA	*c* (%)[a]	ee_p **5** (%)[b]
1	*ArS*TA	<1	<1
2	*ArR*TA	<1	<1
3	*ArR*-mut11	85	47 (*R*)
4	*Vf*TA	<1	<1
5	*VfTA-mut*	<1	<1
6	*Bm*TA	10	11 (*S*)
7	*Bm*TA-mut	13	41 (*S*)
8	*Cv*TA	83	52 (*S*)
9	*At*TA	<1	<1
10	ATA-200	<1	<1
11	ATA-237	22	28 (*S*)
12	ATA-238	15	50 (*S*)
13	ATA-251	<1	<1
14	ATA-254	<1	<1
15	ATA-256	29	84 (*S*)
16	ATA-260	10	>99 (*S*)
17	ATA-303	32	63 (*R*)
18	ATA-412	30	>99 (*R*)
19	ATA-415	20	50 (*R*)
20	ATA-P1-B04	6	40 (*S*)
21	ATA-P2-A01	<1	<1
22	ATA-P2-B01	5	>99 (*R*)
23	ATA-007	5	>99 (*R*)
24	ATA-013	21	56 (*R*)
25	ATA-025	86	60 (*R*)
26	ATA-113	16	>99 (*R*)
27	ATA-117	<1	<1
28	ATA.217	8	40 (*R*)
29	ATA-234	19	5 (*R*)
30	ATA-301	7	>99 (*R*)
31	ATA-P1-F03	32	50 (*S*)
32	ATA-P1-G05	14	>99 (*S*)
33	ATA-P2-A07	4	>99 (*R*)
34	ATA-024	65	9 (*R*)
35	ATA-033	76	50 (*R*)
36	ATA-P1-A06	<1	<1
37	ATA-P1-G06	<1	<1

[a] Conversion values were calculated by reverse phase HPLC using calibration lines (see section IV).

[b] Enantiomeric excess values of the resulting amine were measured by HPLC analyses after derivatization of the reaction crude with methoxyacetyl chloride (4 µL) in the presence of pyridine (2 µL) and dichloromethane (0.5 mL) as a solvent (see section IV).

III. Bioreduction experiments

Table S2. Bioreduction of ketone **4** (25 mM) in Tris-HCl buffer (50 mM, pH 7.5) with 2-PrOH as a cosolvent (10% vol) after 24 h at 30 °C and 250 rpm.

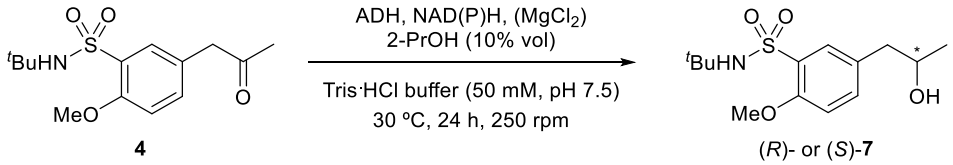

Entry	ADH	Cofactor	$MgCl_2$	*c* (%)[a]	ee_p **7** (%)[b]
1	ADH-A	NADH	NO	91	>99 (*S*)
2	*Tes*ADH	NADH	NO	<1	---
3	*Sy*ADH	NADH	NO	<1	---
4	ADH-T	NADPH	NO	<1	---
5	*Ras*ADH	NADPH	NO	<1	---
6	*Lb*ADH	NADPH	YES	<1	---
7	evo.1.1.200	NADH	YES	> 99	> 99 (*R*)
8	KRED-P1-A04	NADPH	YES	<1	---
9	KRED-P1-A12	NADPH	YES	72	>99 (*R*)
10	KRED-P1-B05	NADPH	YES	50	>99 (*R*)
11	KRED-P1-C01	NADPH	YES	>99	89 (*R*)
12	KRED-P1-H08	NADPH	YES	<1	---
13	KRED-P2-B02	NADPH	YES	>99	81 (*S*)
14	KRED-P2-C02	NADPH	YES	>99	87 (*S*)
15	KRED-P2-C11	NADPH	YES	<1	---
16	KRED-P2-D03	NADPH	YES	94	51 (*R*)
17	KRED-P2-D11	NADPH	YES	>99	72 (*R*)
18	KRED-P2-D12	NADPH	YES	43	39 (*R*)
19	KRED-P2-G03	NADPH	YES	<1	---
20	KRED-P2-H07	NADPH	YES	94	>99 (*R*)
21	KRED-P3-B03	NADPH	YES	>99	92 (*S*)
22	KRED-P3-H12	NADPH	YES	>99	29 (*S*)

[a] Conversion values were calculated by HPLC using calibration curves (see section IV).
[b] Enantiomeric excess values were calculated using HPLC and a chiral stationary phase (see section IV).

IV. Analytical data

IV.1. General procedures for the synthesis of racemic amides for the determination of the enantiomeric excess of the amine 5

Once the racemic amine **5** was isolated, it was chemically acylated to obtain the corresponding racemic amides **6a** and **6b**, which are the final products of the enzymatic resolution reactions depending on the use of EtOAc or ethyl methoxyacetate ($MeOCH_2CO_2Et$). Thus, by reaction with the corresponding acid chlorides in the presence of pyridine as a base and dichloromethane as a solvent, the corresponding acetamide **6a** and methoxyacetamide **6b** were obtained both in racemic form with 88% and 76% isolated yield. This allowed the development of analytical methods using the HPLC technique with chiral columns to calculate the enantiomeric excesses of the amines and amides obtained in the studied biotransformation (see section IV).

IV.1.1. General procedure for the acylation of racemic amine 5 as *N*-(1-{3-[*N*-(*tert*-butyl)sulfamoyl]-4-methoxyphenyl}propan-2-yl)acetamide (*rac*-6a)

Pyridine (9.90 µL, 0.121 mmol) and methoxyacetyl chloride (17.0 µL, 0.24 mmol) were added to a solution of the racemic amine **5** (29.3 mg, 0.097 mmol, 0.2 M) in CH_2Cl_2 (0.61 mL) inside a Schlenk flask and under nitrogen atmosphere. The mixture was stirred at room temperature for 3 h, at which time the disappearance of the starting product was observed by TLC analysis (5% MeOH/CH_2Cl_2). The solvent was distilled under reduced pressure, and the reaction crude was purified through column chromatography on silica gel (5% MeOH/CH_2Cl_2), obtaining the racemic amide **6a** (31.2 mg, 88% yield) as a green solid. R_f (5% MeOH/CH_2Cl_2): 0.50. Mp 90-92 °C. IR ν 3380, 3199, 2925, 1661, 1494, 1301, 1141, 1070, 823, 557, 491 cm^{-1}. ^1H NMR (300.13 MHz, $CDCl_3$) δ 7.71 (d, J = 2.2 Hz , 1H), 7.38 (dd, J = 8.5, 2.2 Hz, 1H), 6.98 (d, J = 8.5 Hz, 1H), 5.39 (d, J = 8, 2 Hz, 1H), 4.95 (s, 1H), 4.24–3.99 (m, 1H), 3.99 (s, 3H), 2.76 (quintd, J = 13.6, 6 .6 Hz, 2H), 1.94 (s, 3H), 1.19 (s, 9H), 1.10 (d, J = 6.7 Hz, 3H). ^{13}C NMR (75.5 MHz, $CDCl_3$) δ 169.5 (C), 154.5 (C), 134.6 (CH), 130.9 (C), 130.7 (C), 129.8 (CH), 112.4 (CH), 56.3 (CH), 54.4 (CH), 46.3 (CH), 41.3 (CH_2), 30.0 (3 CH_3), 23.4 (CH_3), 20.0 (CH_3). HRMS (ESI^+): m/z calcd for $C_{16}H_{26}N_2NaO_4S$: 365.1505 $[M+Na]^+$; found: 365.1490.

IV.1.2. General procedure for the acylation of racemic amine 5 as *N*-(1-{3-[*N*-(*tert*-butyl)sulfamoyl]-4-methoxyphenyl}propan-2-yl)methoxyacetamide (*rac*-6b)

Pyridine (16.8 µL, 0.208 mmol) and methoxyacetyl chloride (37. 9 µL, 0.42 mmol) were added to a solution of the racemic amine **5** (50.0 mg, 0.166 mmol) in CH_2Cl_2 (0.83 mL) inside a Schlenk flask under an inert atmosphere. The solution was stirred at room temperature for 3 h, at which time the disappearance of the starting amine was observed by TLC analysis (5% MeOH/CH_2Cl_2). The solvent was distilled under reduced pressure, and the reaction crude was purified through column chromatography on silica gel (5% MeOH/CH_2Cl_2), obtaining the racemic methoxyacetamide **6b** (47.3 mg, 76% yield) as a green solid. R_f (5% MeOH/CH_2Cl_2): 0.45. Mp 94-96 °C. IR ν 3380, 2967, 1661, 1495,1142, 558 cm^{-1}. ^1H NMR (300.13 MHz, $CDCl_3$) δ 7.70 (d, J = 2.0 Hz, 1H), 7.36 (dd, J = 8.4, 2.0 Hz, 1H), 6.96 (d, J = 8.5 Hz, 1H), 4.97 (s , 1H), 3.97 (s, 3H), 3.82 (d, J = 4.9 Hz, 2H), 3.38 (s, 3H), 2.78 (quintd, J = 13.7, 6.6 Hz, 2H), 1.93 (s, 1H), 1.17 (s, 9H), 1.12 (d, J = 6.6 Hz, 3H). ^{13}C NMR (75.5 MHz, $CDCl_3$) δ 168.8 (C), 154.6 (C), 134.6 (CH), 130.8 (C), 130.7 (C), 129.8 (CH), 112.3 (CH), 71.8 (CH_2), 59.2 (CH), 56.3 (CH), 54.3 (C), 45.5 (CH), 41.4 (CH_2), 30.0 (3 CH_3), 19.9 (CH_3). HRMS (ESI^+): m/z calcd for $C_{17}H_{28}N_2NaO_5S$: 395.1611 $[M+Na]^+$; found: 395.1599.

IV.2. HPLC analysis for the determination of product percentages and ee values of selected compounds

HPLC analyses were employed for the determination of the conversion and the enantiomeric excess values of organic compounds obtained after different biotransformations such as lipase-catalyzed acylation of the racemic amine **5**, ketone **4** bioreduction or ketone **4** biotransamination.

IV.2.1. Analytics for lipase-catalyzed reactions

For the determination of conversions (*c*) and enantiomeric excesses (*ee*) of substrates and products from enzymatic reactions **using lipases**, the HPLC technique was used after *in situ* derivatization of the reaction crudes (Table S3).

Table S3. Retention times for the determination of conversion and enantiomeric excess values.

Entry	Substrate[a]	Retention time (min)	
1	Acetamide **6a**	9.0 (*R*)	12.3 (*S*)
2	Methoxyacetamide **6b**	18.2 (*R*)	26.8 (*S*)

[a] The resulting peaks for the unprotected amine **5** were very wide with an overlap found between both enantiomers. Thus, chemical derivatization processes were necessary to measure the enantiomeric excess values of the optically active amine obtained after the studied biotransformations.

A Hewlett Packard 1100 chromatograph with a UV detector and the chiral column Chiralpak AD-H (4.6 mm diameter x 25 cm length, x 5 µm particle size) from Daicel was employed. Detection was performed at a wavelength (λ) of 210 nm and a column temperature of 30 °C, using a Hexane:2-PrOH (85:15 *v*/*v*) mixture as the eluent with a flow rate of 1.0 mL/min:

- The analyses of pure compound samples, both racemic and optically active ones, were performed by injecting samples at a concentration of 1 mg/mL in the Hexane:2-PrOH (85:15 *v*/*v*) mixture.
- For the monitorization of the biotransformations, reaction aliquots (20 µL) were taken every 24 h and diluted in 980 µL of the Hexane:2-PrOH (85:15 *v*/*v*) mixture.

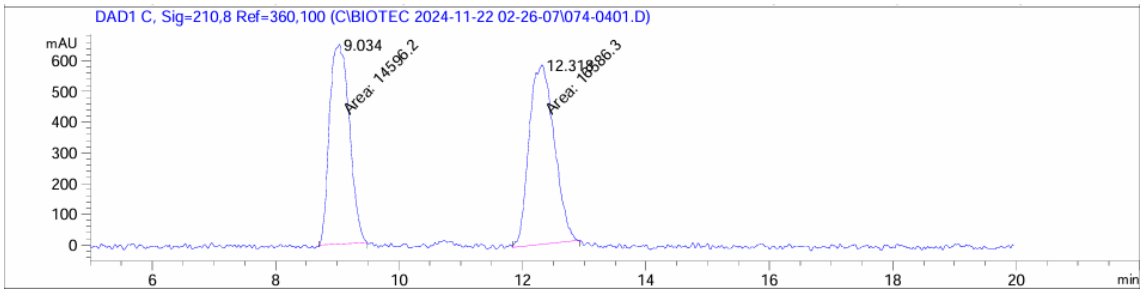

Figure S2. HPLC chromatogram of racemic acetamide **6a** [Chiralpak AD-H, 30 ºC, 210 nm and Hexane:2-PrOH (85:15 *v*/*v*) at 1.0 mL/min].

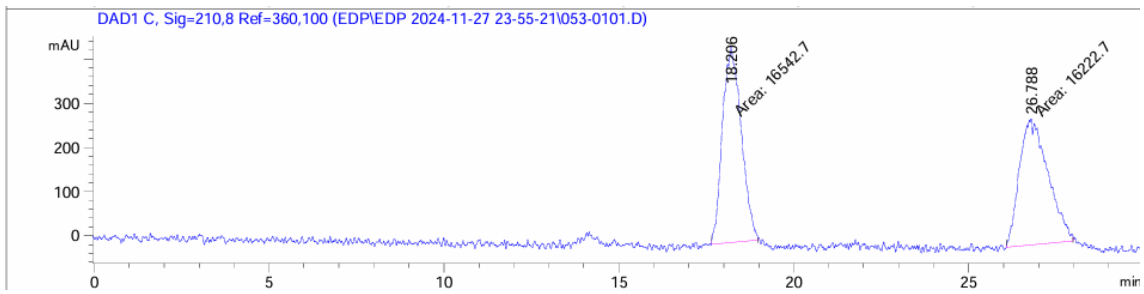

Figure S3. HPLC chromatogram of racemic methoxyacetamide **6b** [Chiralpak AD-H, 30 ºC, 210 nm and Hexane:2-PrOH (85:15 *v*/*v*) at 1.0 mL/min].

IV.2.2. Analytics for ADH-catalyzed reactions

The HPLC technique was also used for the determination of conversions and enantiomeric excesses when using **alcohol dehydrogenases** (Table S4 and Figure S4). A Hewlett Packard 1100 chromatograph with a UV detector and the chiral column Chiralpak OJ-H (4.6 mm diameter x 25 cm length x 5 µm particle size) from Daicel was employed. Detection was performed at a wavelength (λ) of 210 nm and a column temperature of 40 °C, using a Hexane:2-PrOH (85:15 *v*/*v*) mixture as the eluent with a flow rate of 1.0 mL/min.

Table S4. Retention times for the determination of conversion and enantiomeric excess values.

Entry	Substrate	Retention time (min)	
1	Ketone **4**	29.4	
2	Alcohol **7**	11.5 (*R*)	13.1 (*S*)

The conversions were calculated using a calibration curve of the starting ketone (Figure S4).

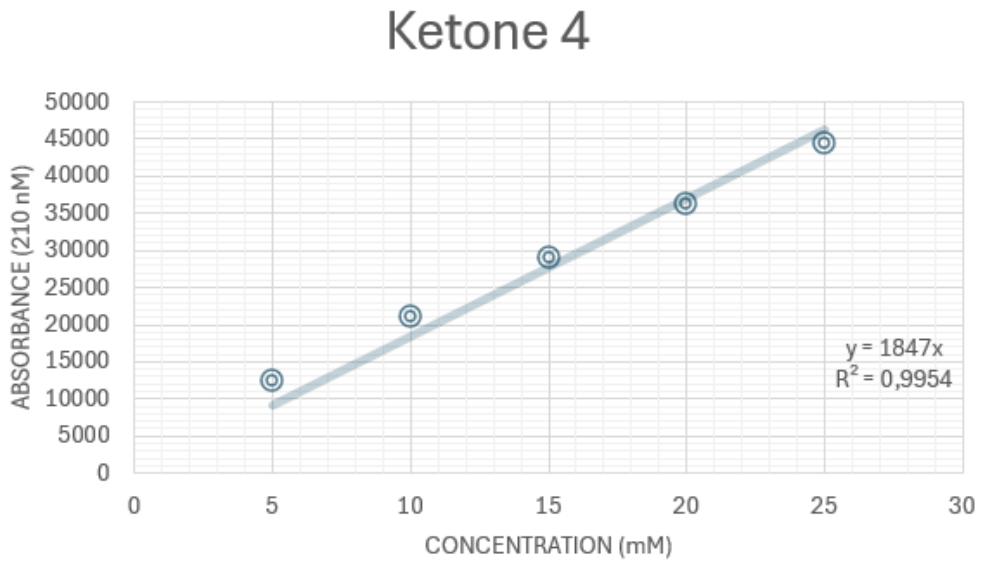

Figure S4. Calibration curve of ketone **4** using normal phase HPLC for bioreduction experiments.

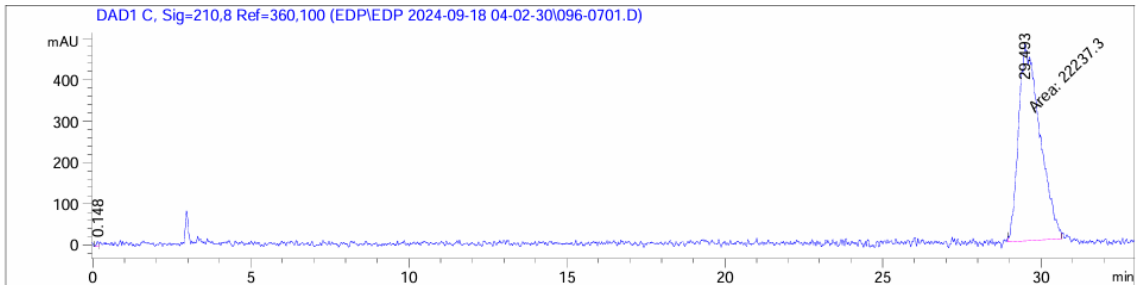

Figure S5. HPLC chromatogram of ketone **4** [Chiralpak OJ-H, 40 ºC, 210 nm and Hexane:2-PrOH (85:15 *v*/*v*) at 1.0 mL/min].

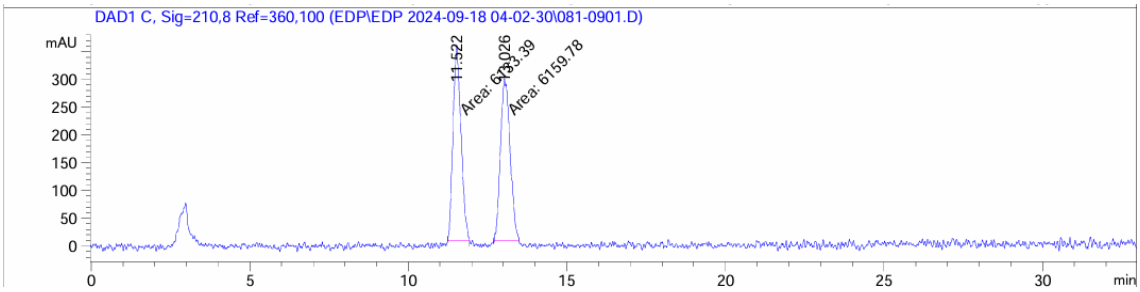

Figure S6. HPLC chromatogram of racemic alcohol **7** [Chiralpak OJ-H, 40 ºC, 210 nm and Hexane:2-PrOH (85:15 *v*/*v*) at 1.0 mL/min].

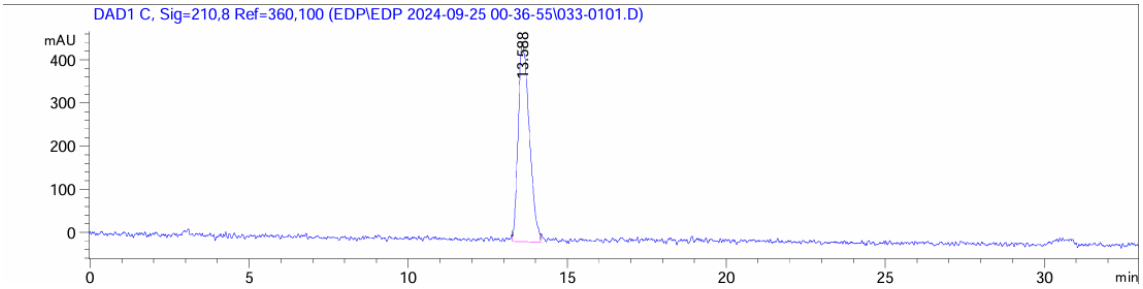

Figure S7. HPLC chromatogram of enantiopure alcohol (*S*)-**7** obtained via bioreduction of ketone **4** using the ADH from *Rhodococcus ruber* overexpressed in *E. coli* (*E. coli* ADH-A) [Chiralpak OJ-H, 40 ºC, 210 nm and Hexane:2-PrOH (85:15 *v*/*v*) at 1.0 mL/min].

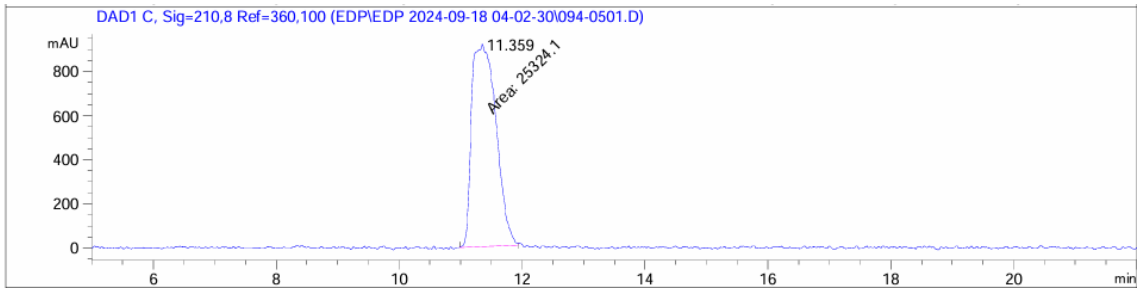

Figure S8. HPLC chromatogram of enantiopure alcohol (*R*)-**7** obtained via bioreduction of ketone **4** using the commercial evo.1.1.200 ADH from [Chiralpak OJ-H, 40 ºC, 210 nm and Hexane:2-PrOH (85:15 *v*/*v*) at 1.0 mL/min].

IV.2.3. Analytics for transaminase-catalyzed reactions

For the monitorization of biotransaminations using **transaminases** (Table S5):

1. The conversions were determined using a reverse phase method employing a calibration curve depicted in Figure S9. An Agilent 1100 series HPLC chromatograph was employed together with a non-chiral Mediterranean SEA18 column (4.6 mm diameter x 25 cm length x 5 µm particle size) from Teknokroma. Detection was performed at a wavelength (λ) of 210 nm and a column temperature of 30 °C, using a MeCN/H_2O (70:30 *v/v*) mixture as the eluent at a flow rate of 1.0 mL/min. Reaction monitoring was carried out at 24 h by injecting a 20 µL aliquot of the obtained reaction crude into 980 µL of the MeCN/H_2O (70:30 *v/v*) mixture.
2. Determination of the *ee* values was carried out following the method already described for lipase-catalyzed reactions using the chiral column Chiralpak AD-H (Table S3).

Table S5. Retention times for the determination of conversion values in biotransaminations.

Entry	Substrate	Retention time (min)
1	Ketone **4**	12.2
2	Amine **5**	2.0

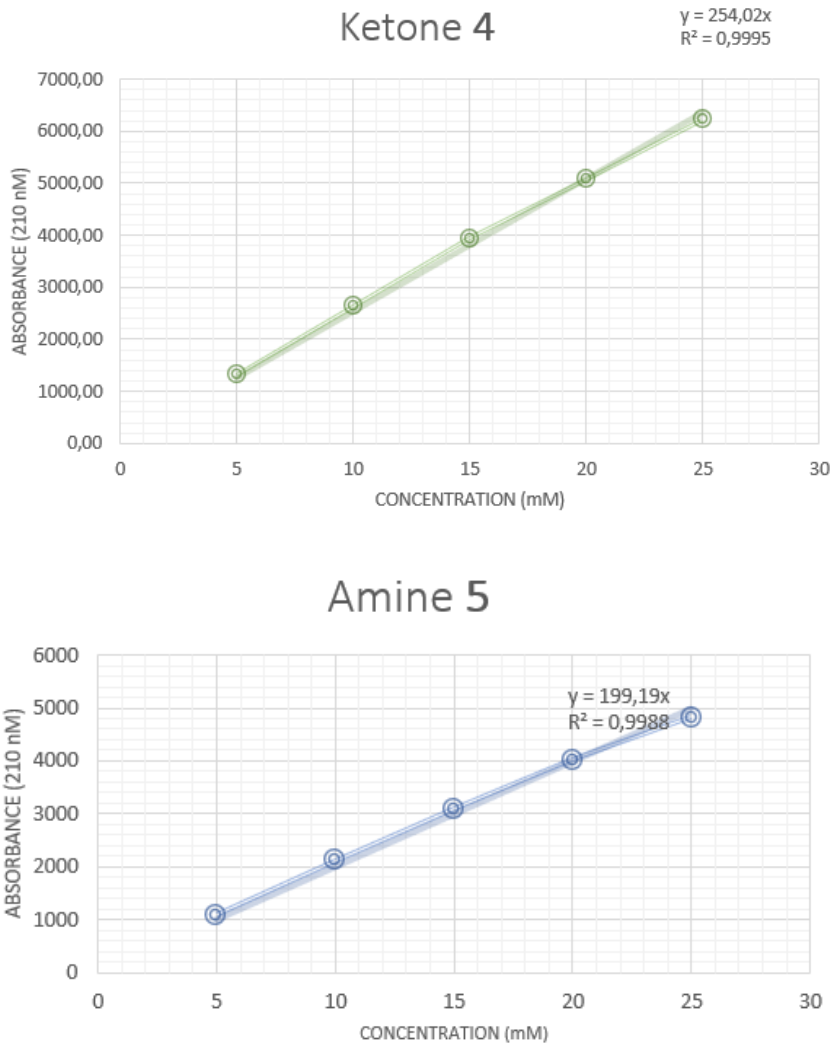

Figure S9. Calibration curves of ketone **4** and amine **5** using reverse-phase HPLC analyses.

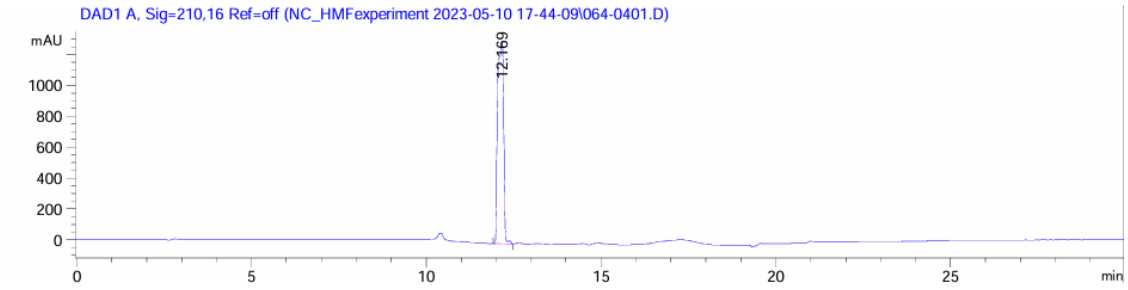

Figure S10. HPLC chromatogram of ketone **4** [Mediterranean SEA18 column, 30 °C, 210 nm, MeCN/H_2O (70:30 *v/v*) mixture at of 1.0 mL/min].

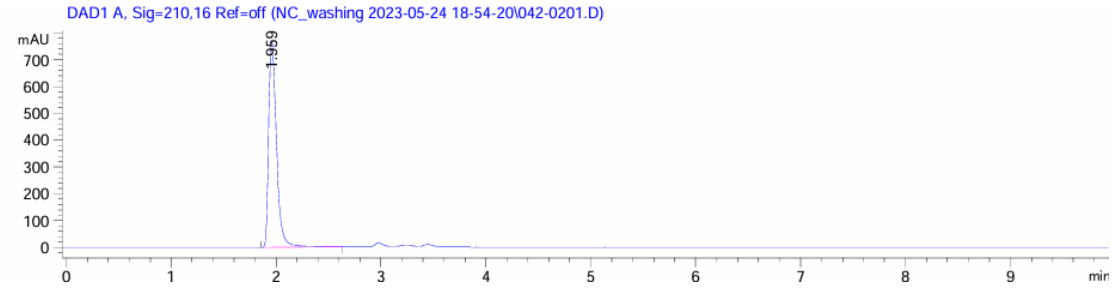

Figure S11. HPLC chromatogram of amine **5** [Mediterranean SEA18 column, 30 °C, 210 nm, MeCN/H_2O (70:30 *v/v*) mixture at of 1.0 mL/min].

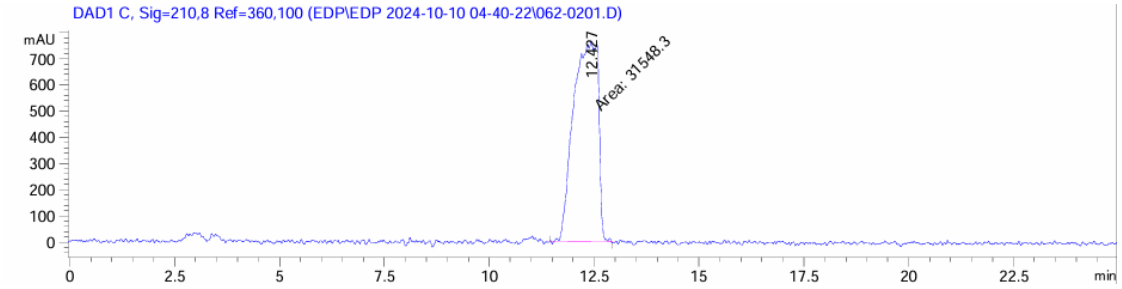

Figure S12. HPLC chromatogram of ketone **4** [Chiralpak AD-H, 30 ºC, 210 nm and Hexane:2-PrOH (85:15 *v/v*) at 1.0 mL/min].

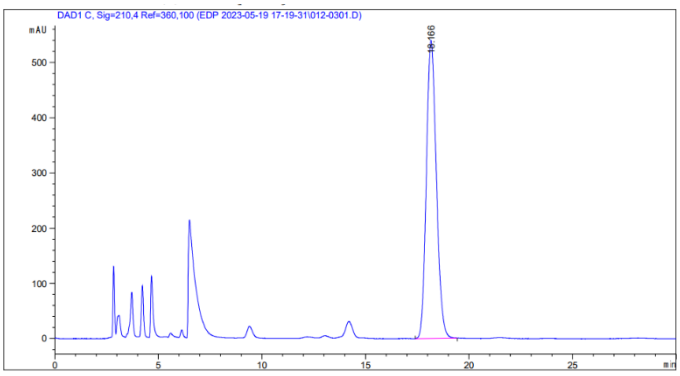

Figure S13. HPLC chromatogram of enantiopure methoxyacetamide (*R*)-**6b** obtained after biotransamination of **4** with ATA-412 and subsequent derivatization [Chiralpak AD-H, 30 ºC, 210 nm and Hexane:2-PrOH (85:15 *v/v*) at 1.0 mL/min]. See Figure S3 for the chromatogram of the racemate).

IV.2.4. Analytics for measurement of the enantiomeric excess of Tamsulosin

For the determination of the enantiomeric excesses value of Tamsulosin, the HPLC technique was used after employing a Hewlett Packard 1100 chromatograph with a UV detector, and the chiral column Chiralpak AD-H (4.6 mm diameter x 25 cm length, x 5 µm particle size) from Daicel was employed. Detection was performed at a wavelength (λ) of 230 nm and a column temperature of 30 °C, using a Hexane:2-PrOH (85:15 *v*/*v*) mixture as the eluent with a flow rate of 1.0 mL/min:

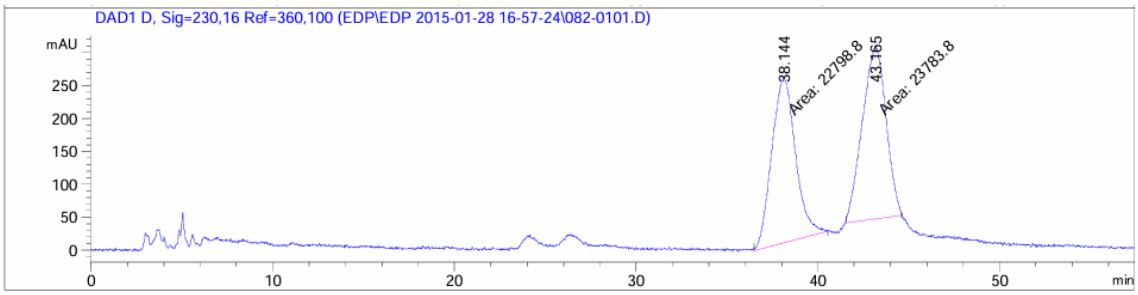

Figure S14. HPLC chromatogram of racemic Tamsulosin (**1**).

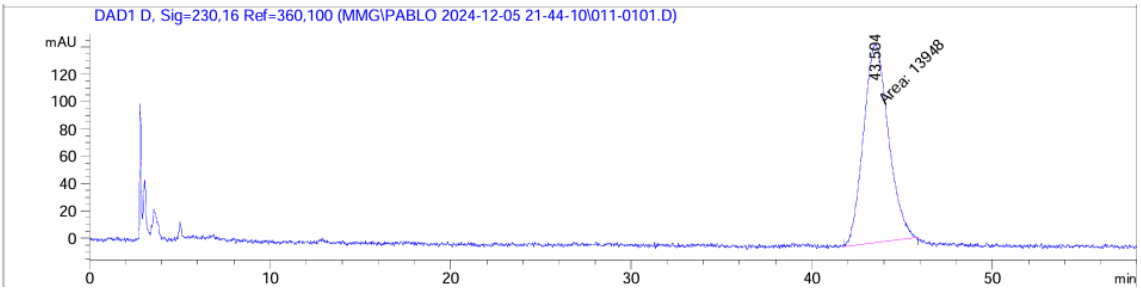

Figure S15. HPLC chromatogram of enantiopure Tamsulosin (*R*)-**1**.

V. NMR spectra

N-(*tert*-butyl)-2-methoxy-5-(2-oxopropyl)benzenesulfonamide (4)

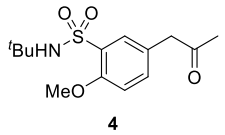

4

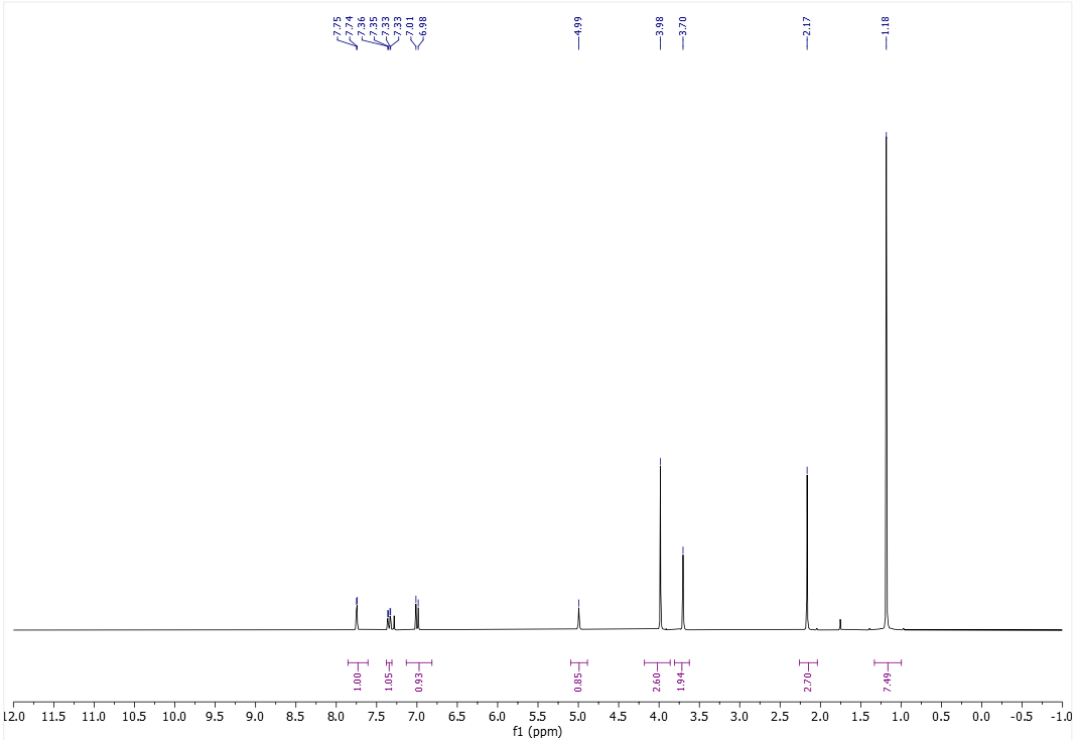

Figure S16. ^{1}H-NMR spectrum ($CDCl_3$) of compound **4**.

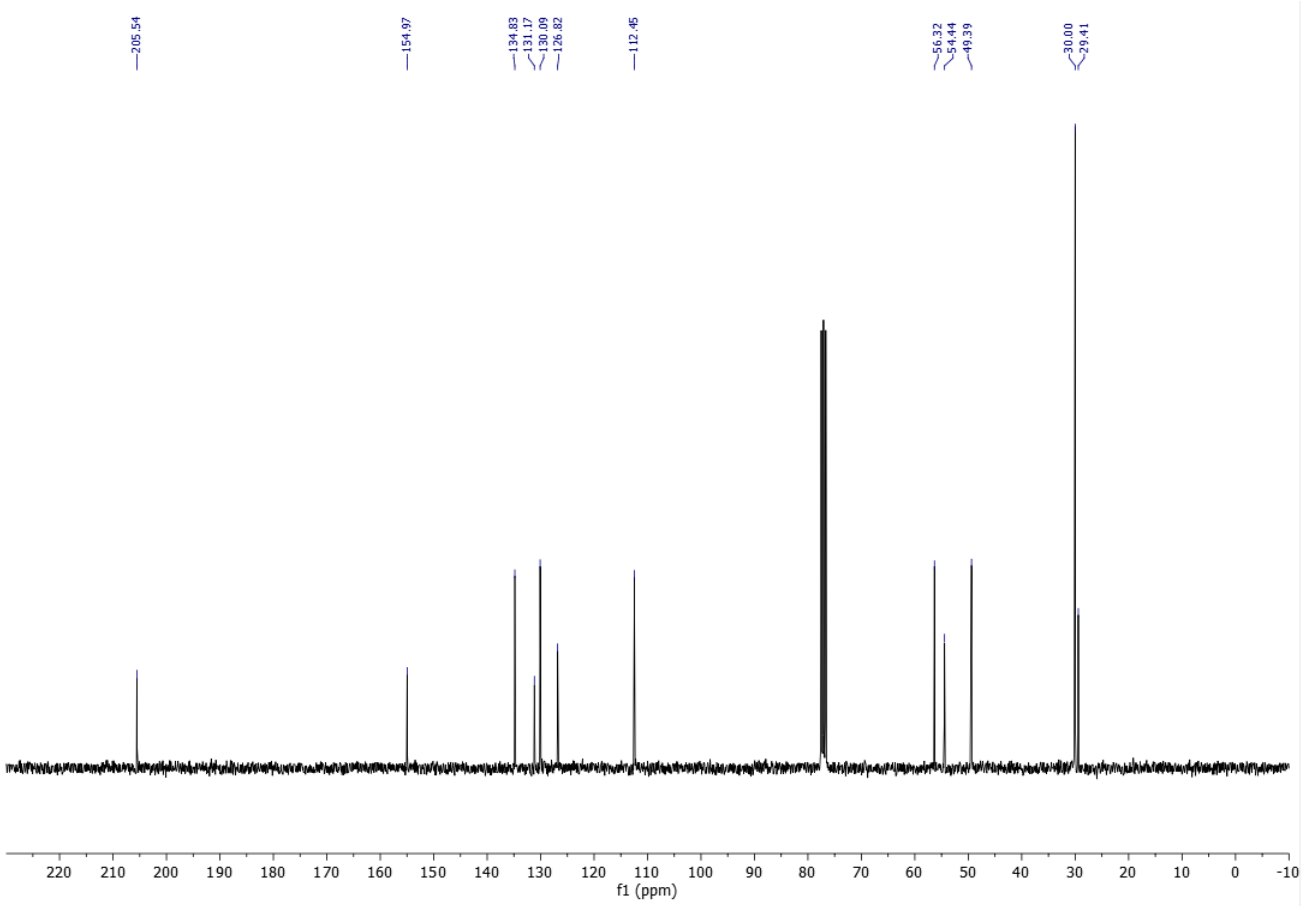

Figure S17. ^{13}C-NMR spectrum ($CDCl_3$) of compound **4**.

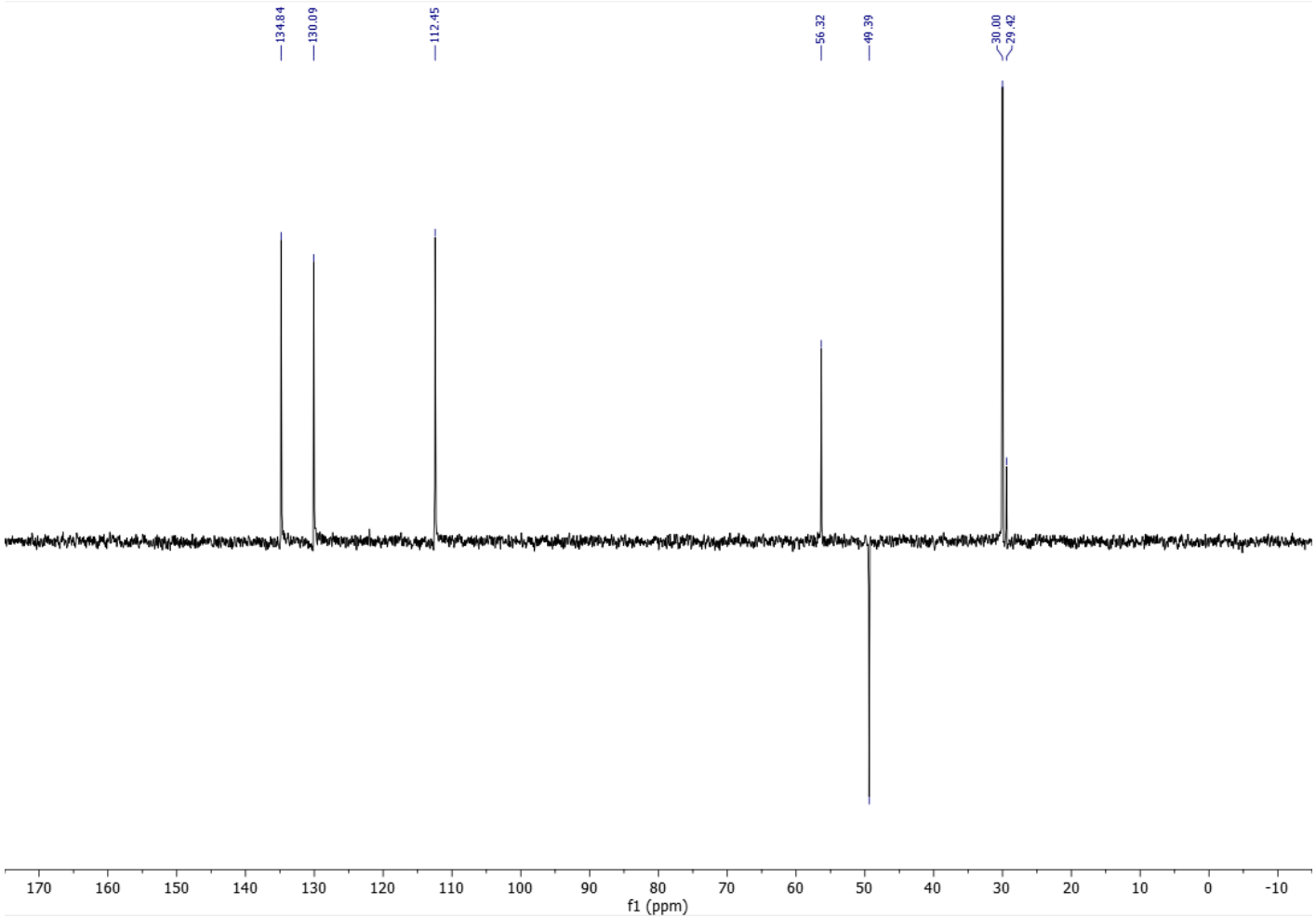

Figure S18. DEPT NMR spectrum ($CDCl_3$) of compound **4**.

5-(2-Aminopropyl)-*N*-(*tert*-butyl)-2-methoxybenzenesulfonamide (5)

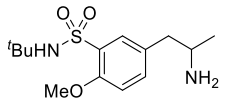

5

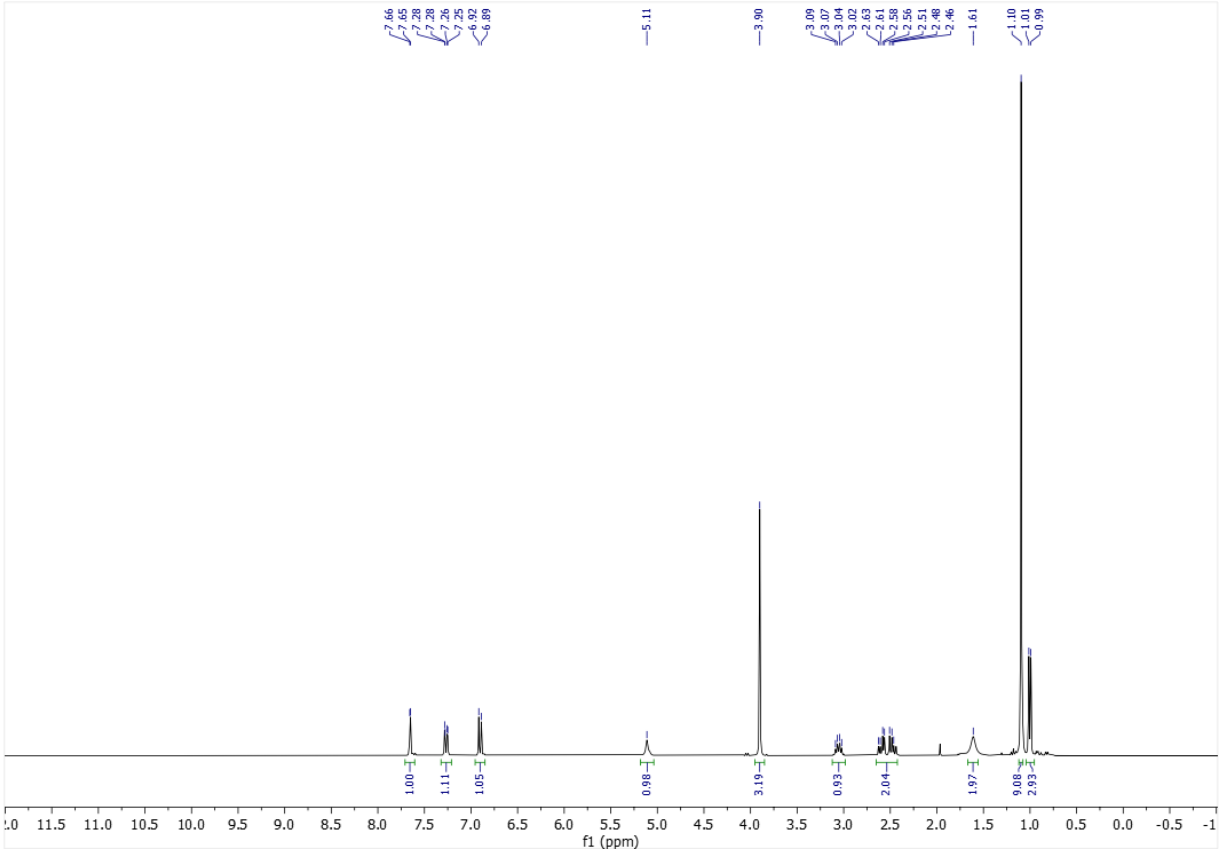

Figure S19. ^{1}H-NMR spectrum ($CDCl_3$) of compound **5**.

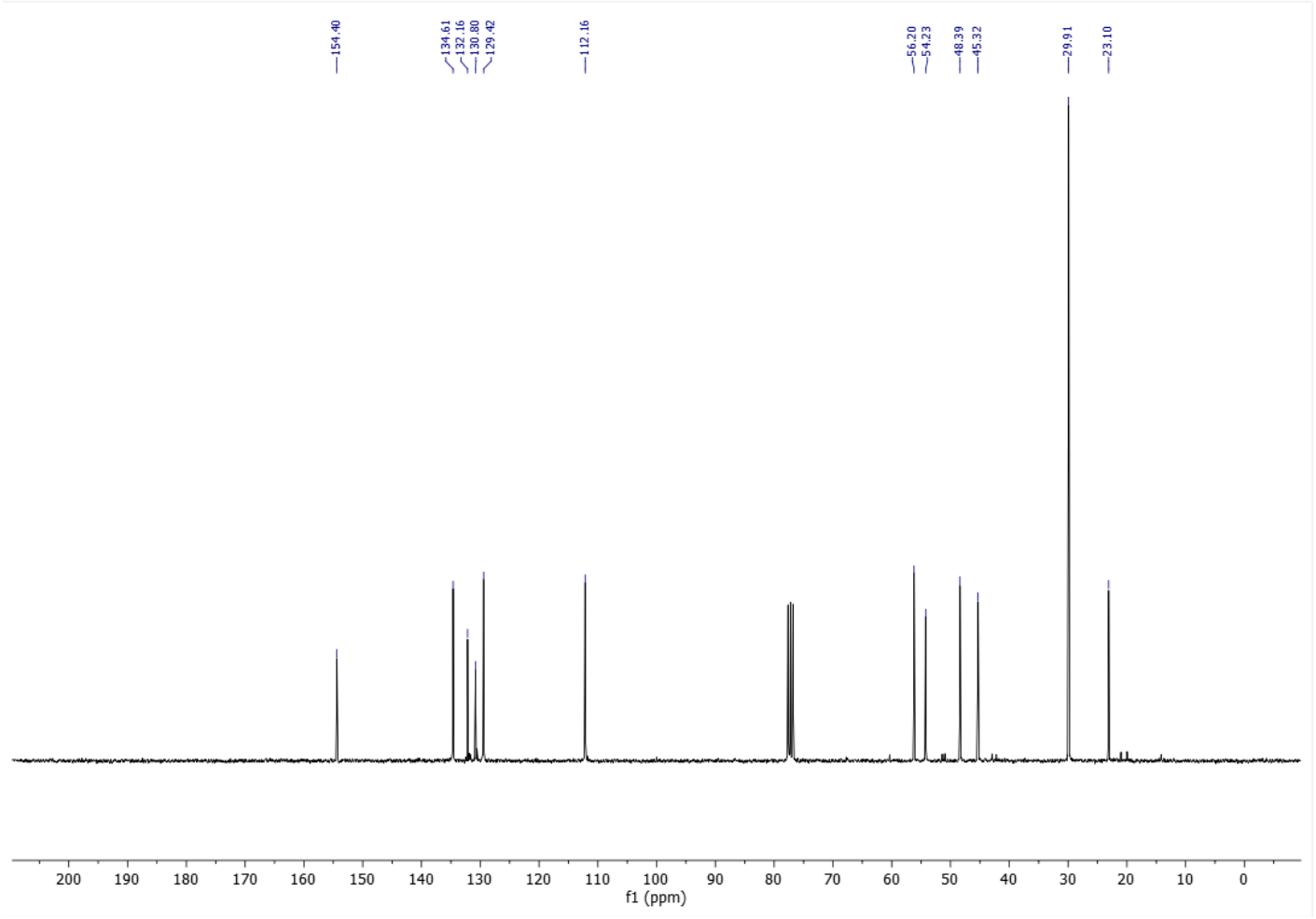

Figure S20. ^{13}C-NMR spectrum ($CDCl_3$) of compound **5**.

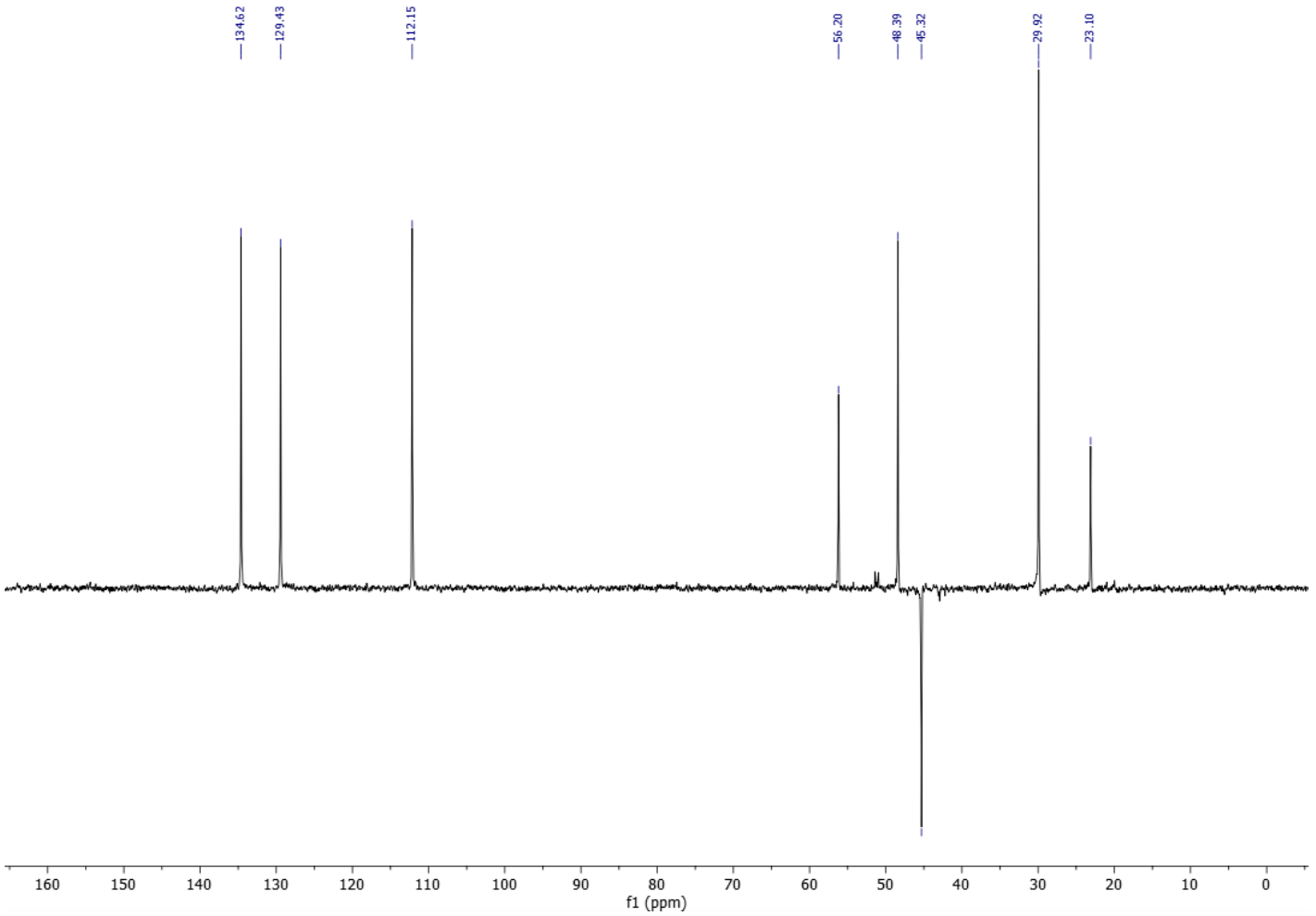

Figure S21. DEPT NMR spectrum ($CDCl_3$) of compound **5**.

***N*-(1-{3-[*N*-(*tert*-butyl)sulfamoyl]-4-methoxyphenyl}propan-2-yl)acetamide (6a)**

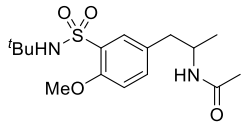

6a

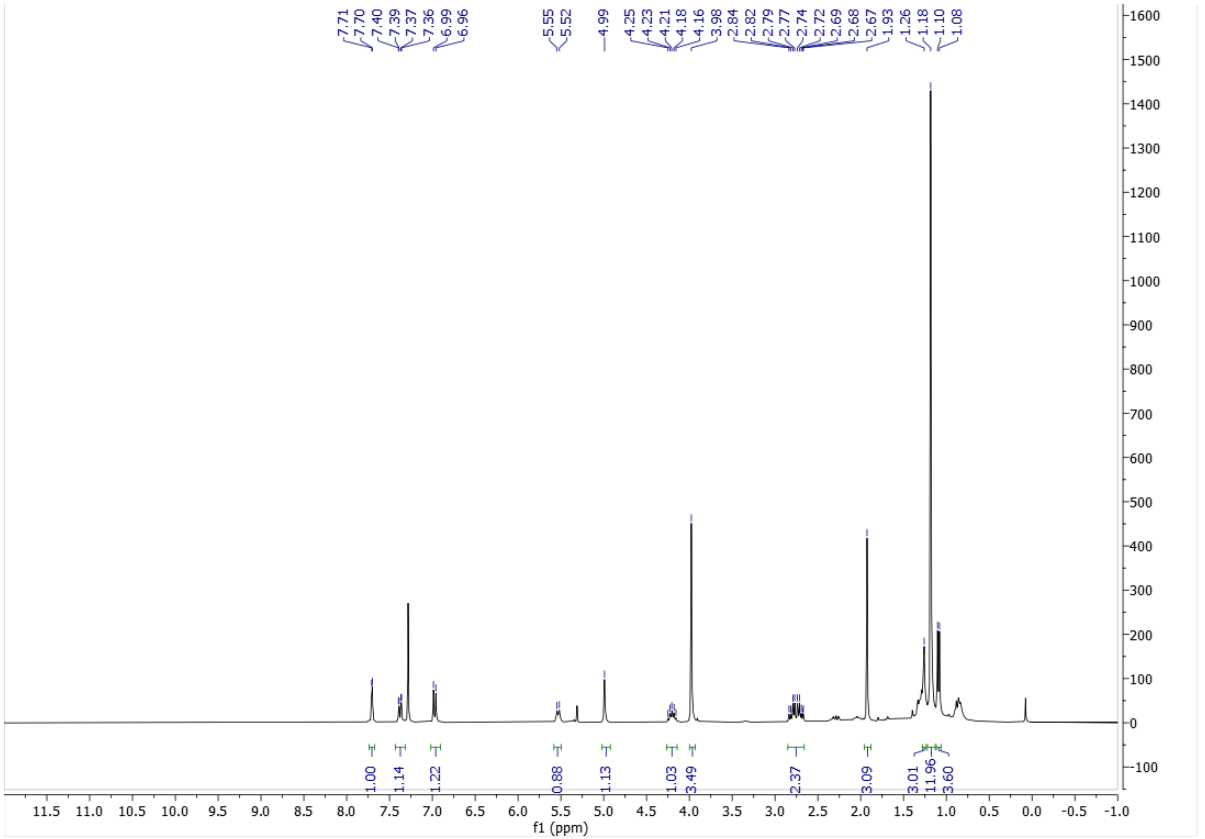

Figure S22. ^{1}H-NMR spectrum ($CDCl_3$) of compound **6a**.

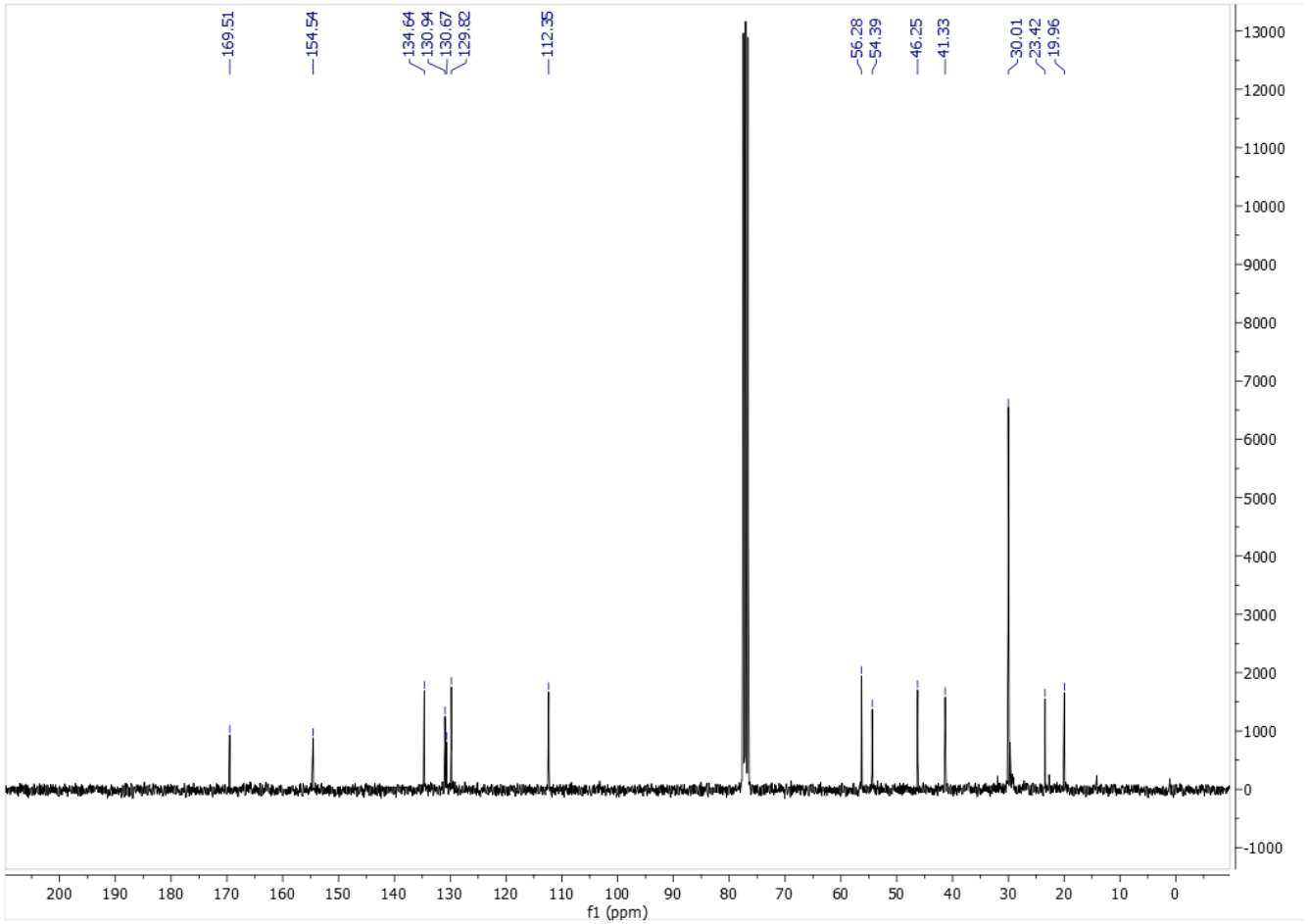

Figure S23. ^{13}C-NMR spectrum ($CDCl_3$) of compound **6a**.

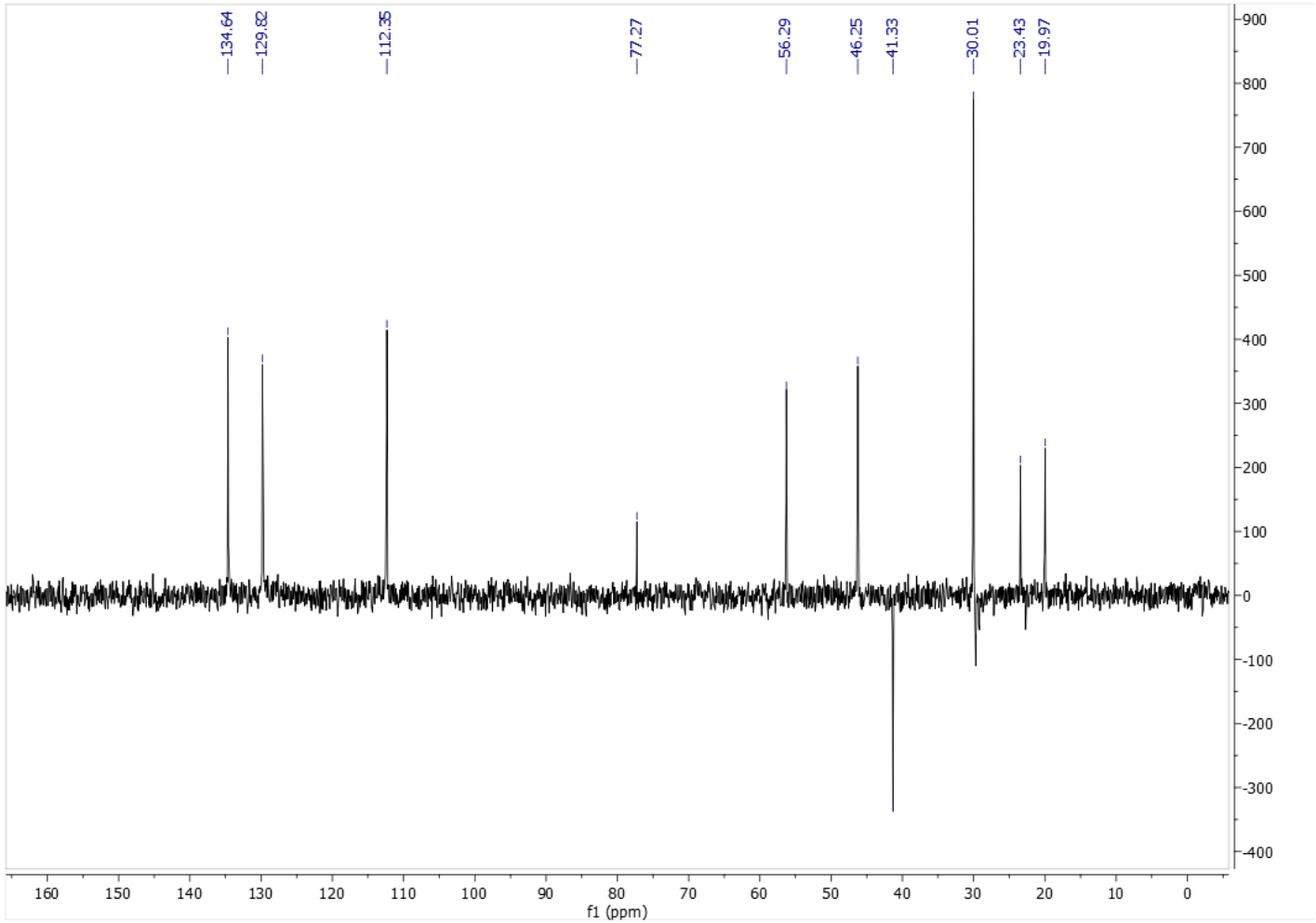

Figure S24. DEPT NMR spectrum ($CDCl_3$) of compound **6a**.

***N*-(1-{3-[*N*-(*tert*-butyl)sulfamoyl]-4-methoxyphenyl}propan-2-yl)methoxyacetamide (6b)**

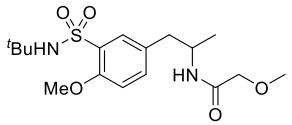

6b

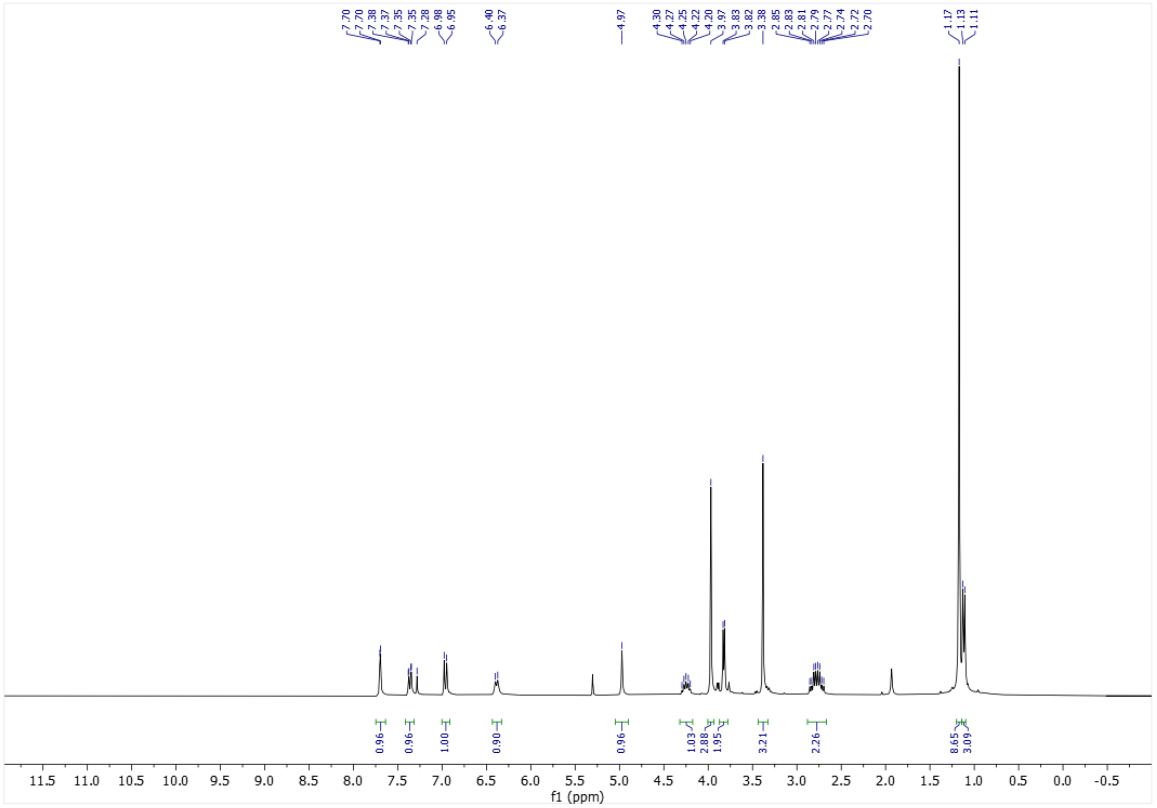

Figure S25. ^{1}H-NMR spectrum ($CDCl_3$) of compound **6b**.

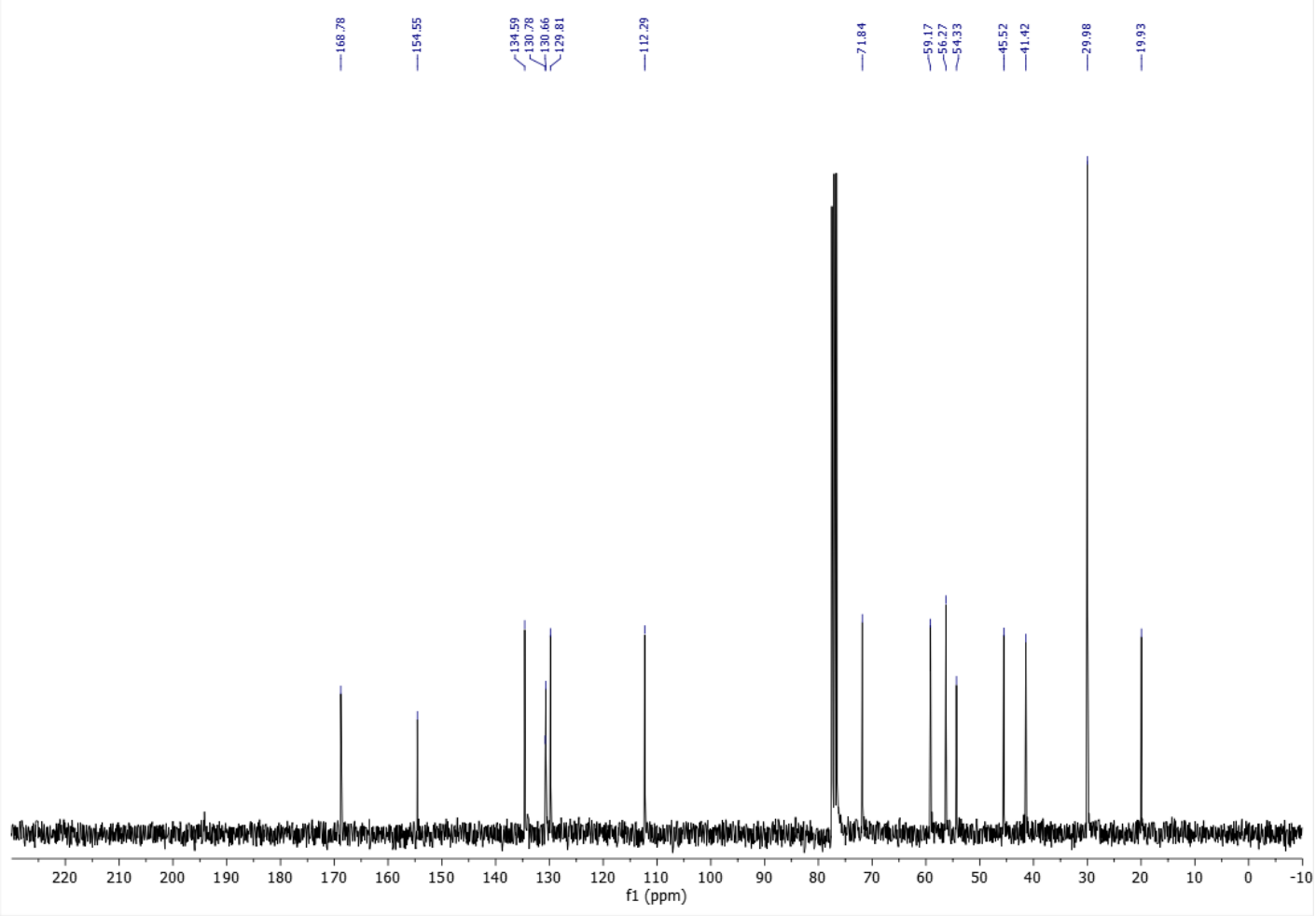

Figure S26. ^{13}C-NMR spectrum ($CDCl_3$) of compound **6b**.

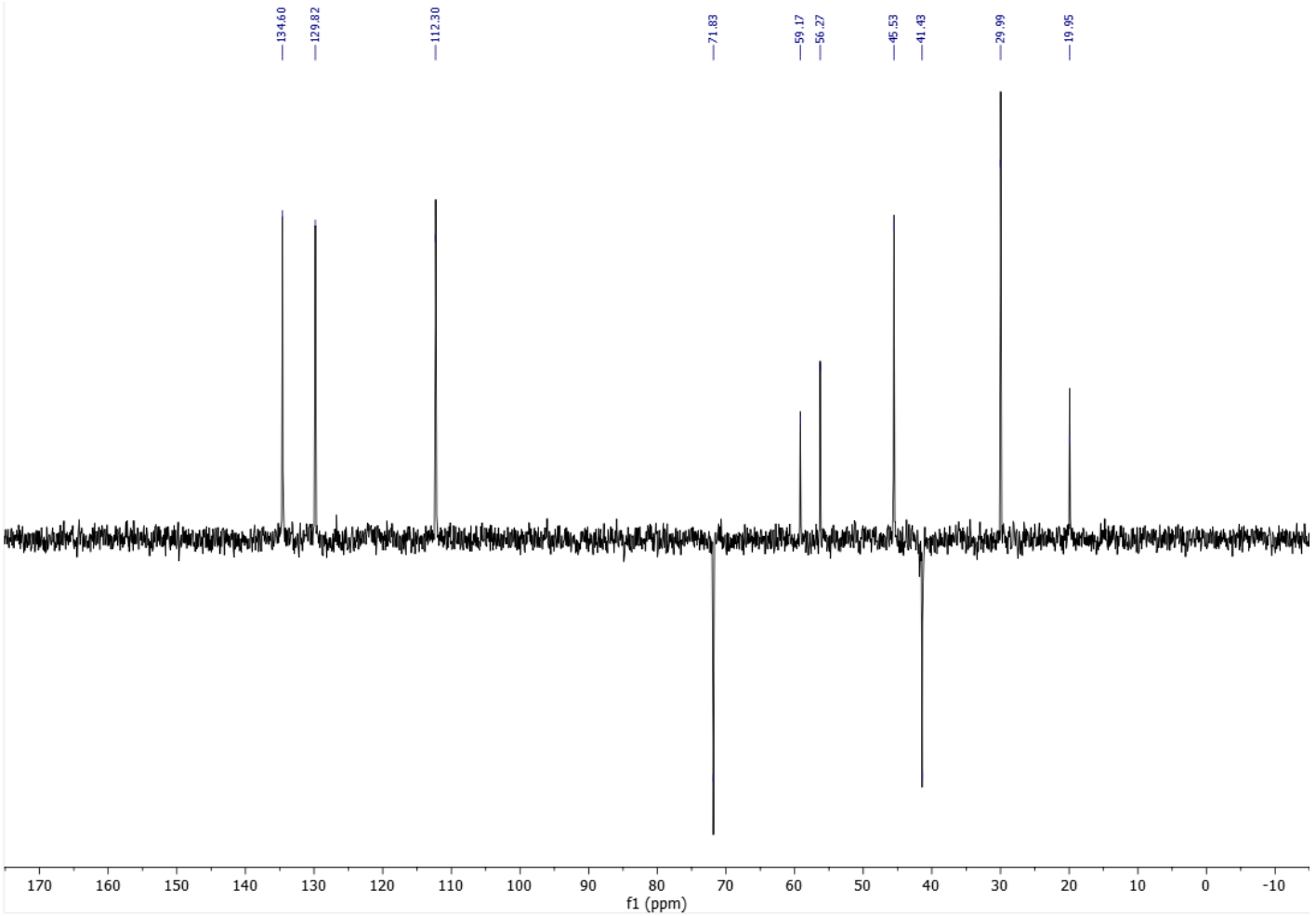

Figure S27. DEPT NMR spectrum ($CDCl_3$) of compound **6b**.

***N*-(*tert*-butyl)-5-(2-hydroxypropyl)-2-methoxybenzenesulfonamide (7)**

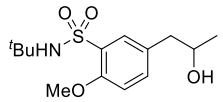

7

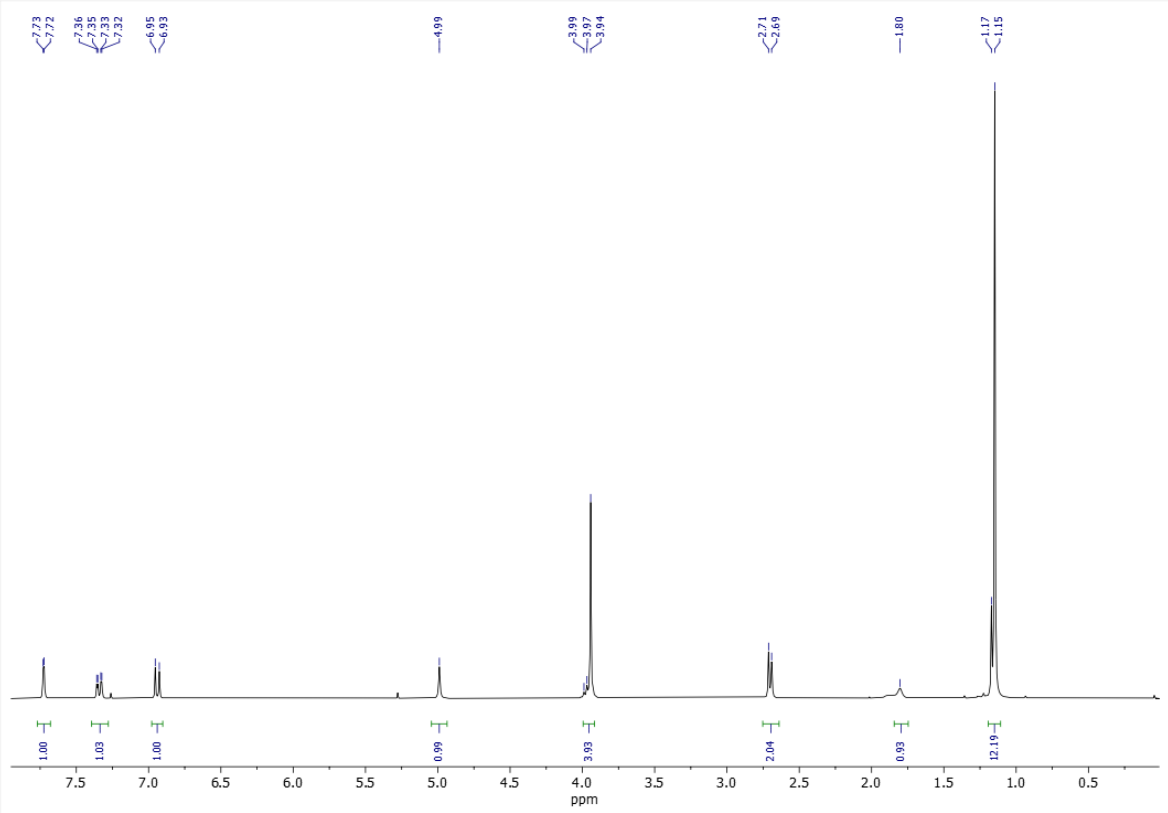

Figure S28. ^{1}H-NMR spectrum ($CDCl_3$) of compound **7**.

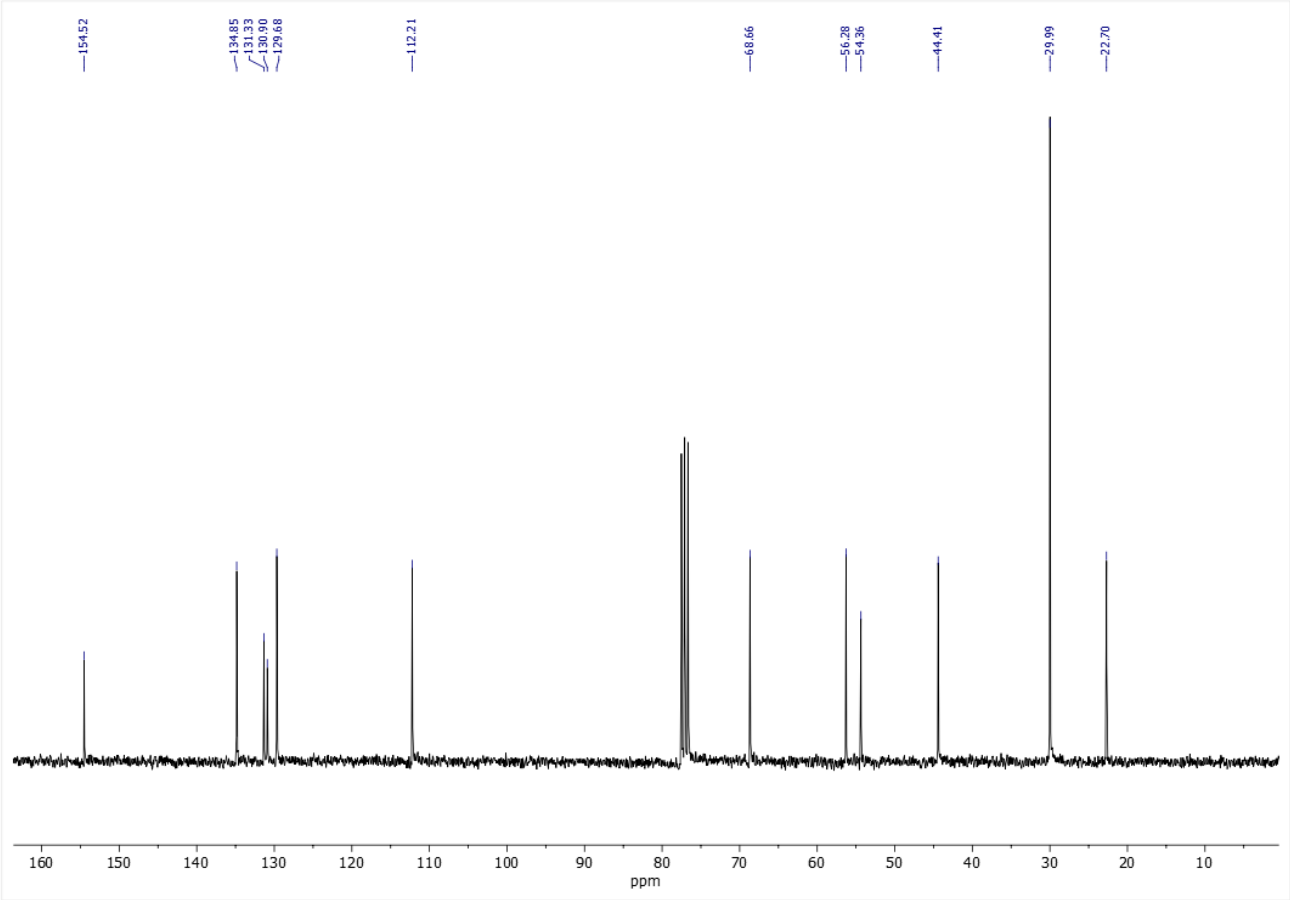

Figure S29. ^{13}C-NMR spectrum ($CDCl_3$) of compound **7**.

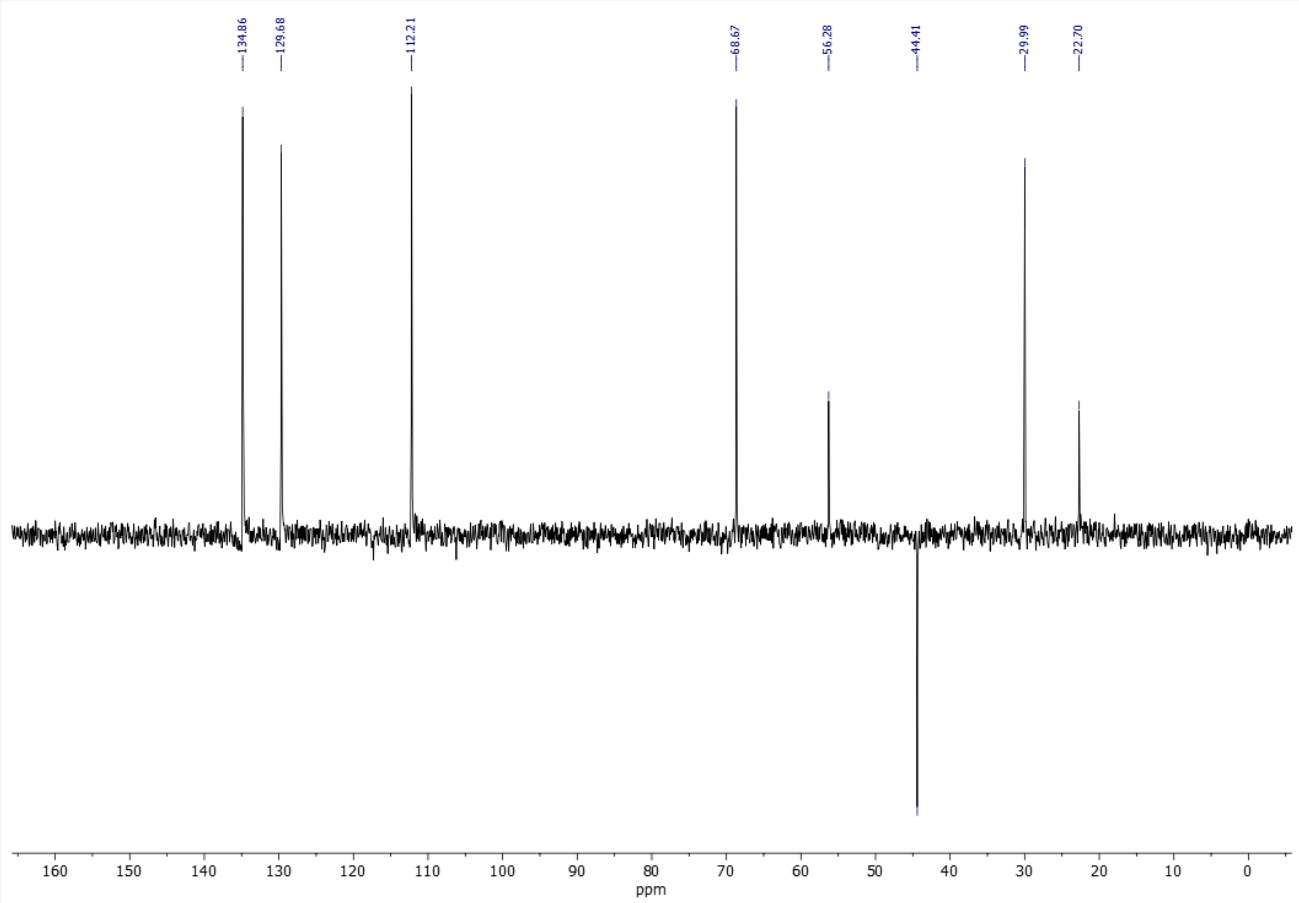

Figure S30. DEPT NMR spectrum ($CDCl_3$) of compound **7**.

2-(2-Ethoxyphenoxy)ethane-1-ol (9)

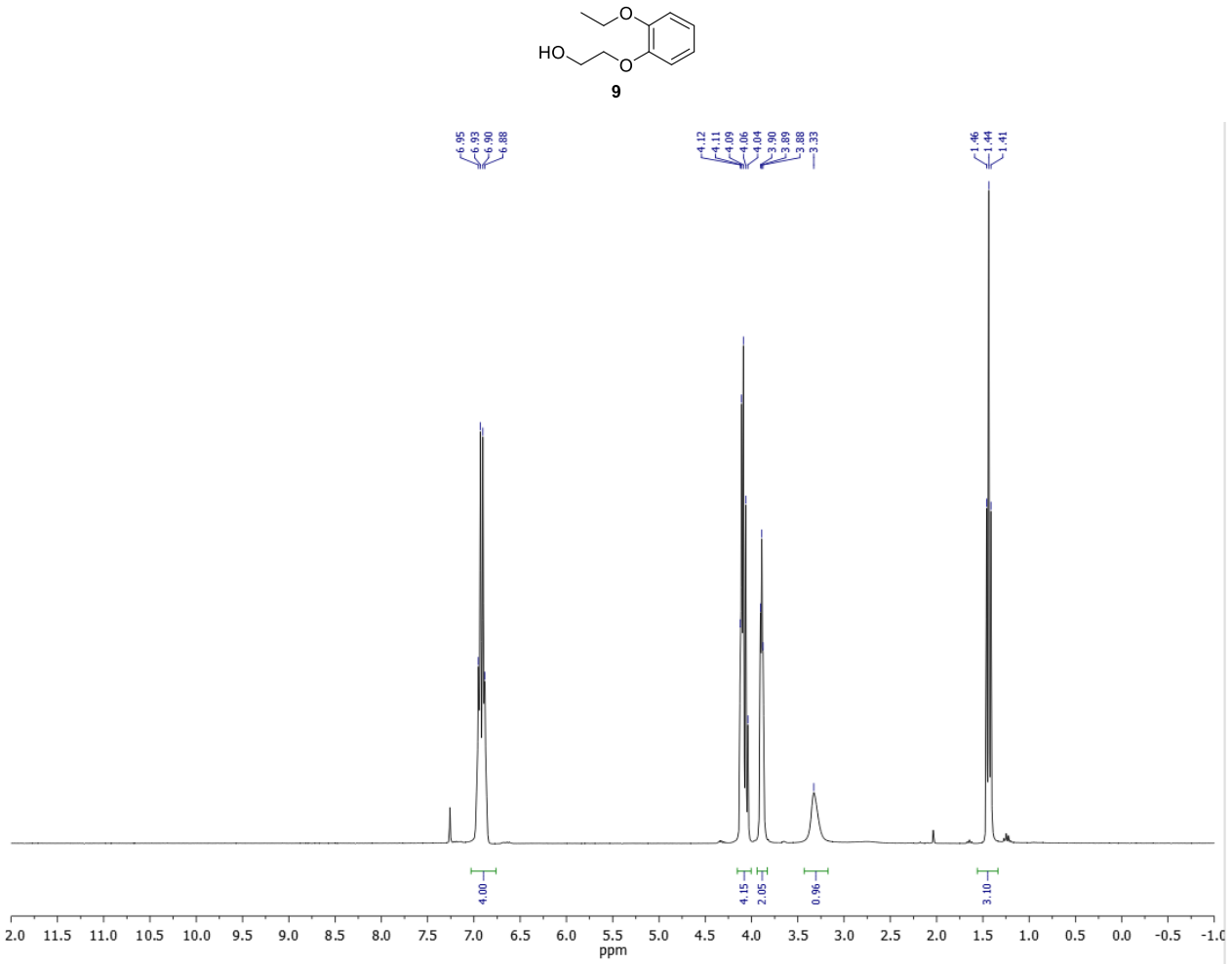

Figure S31. ^{1}H-NMR spectrum ($CDCl_3$) of compound **9**.

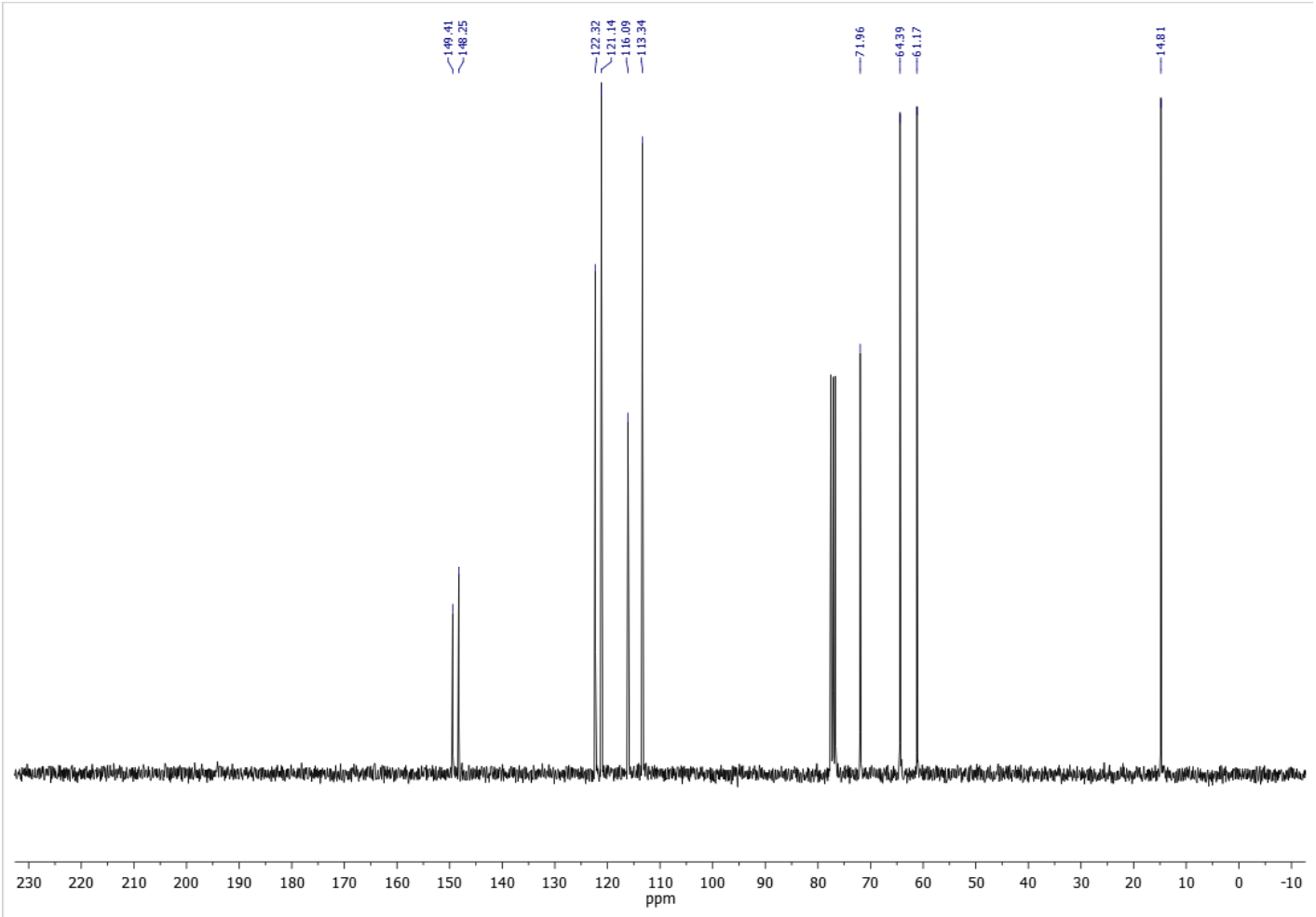

Figure S32. ^{13}C-NMR spectrum ($CDCl_3$) of compound **9**.

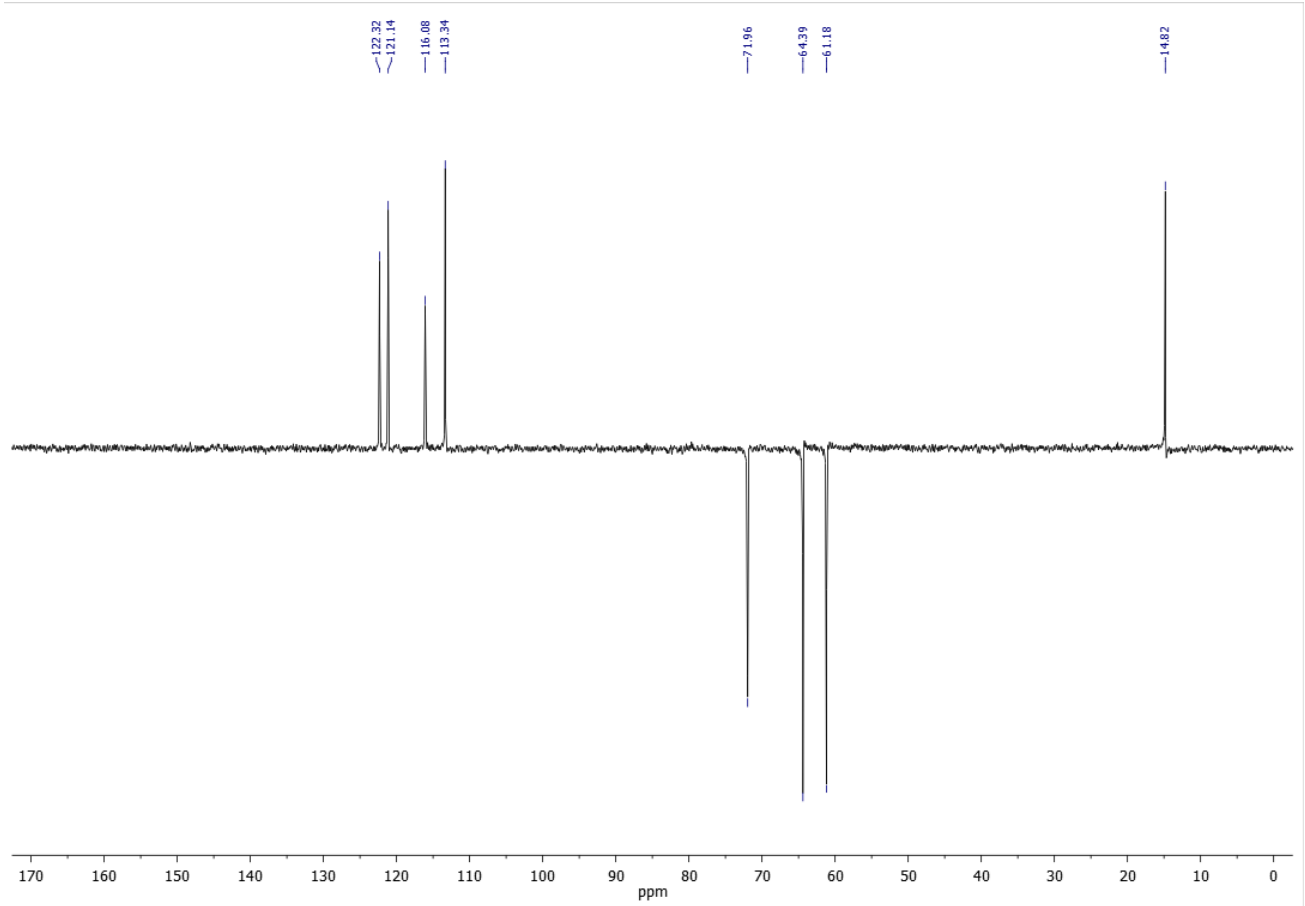

Figure S33. DEPT NMR spectrum ($CDCl_3$) of compound **9**.

2-(2-Ethoxyphenoxy)acetaldehyde (10)

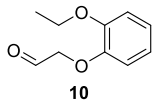

10

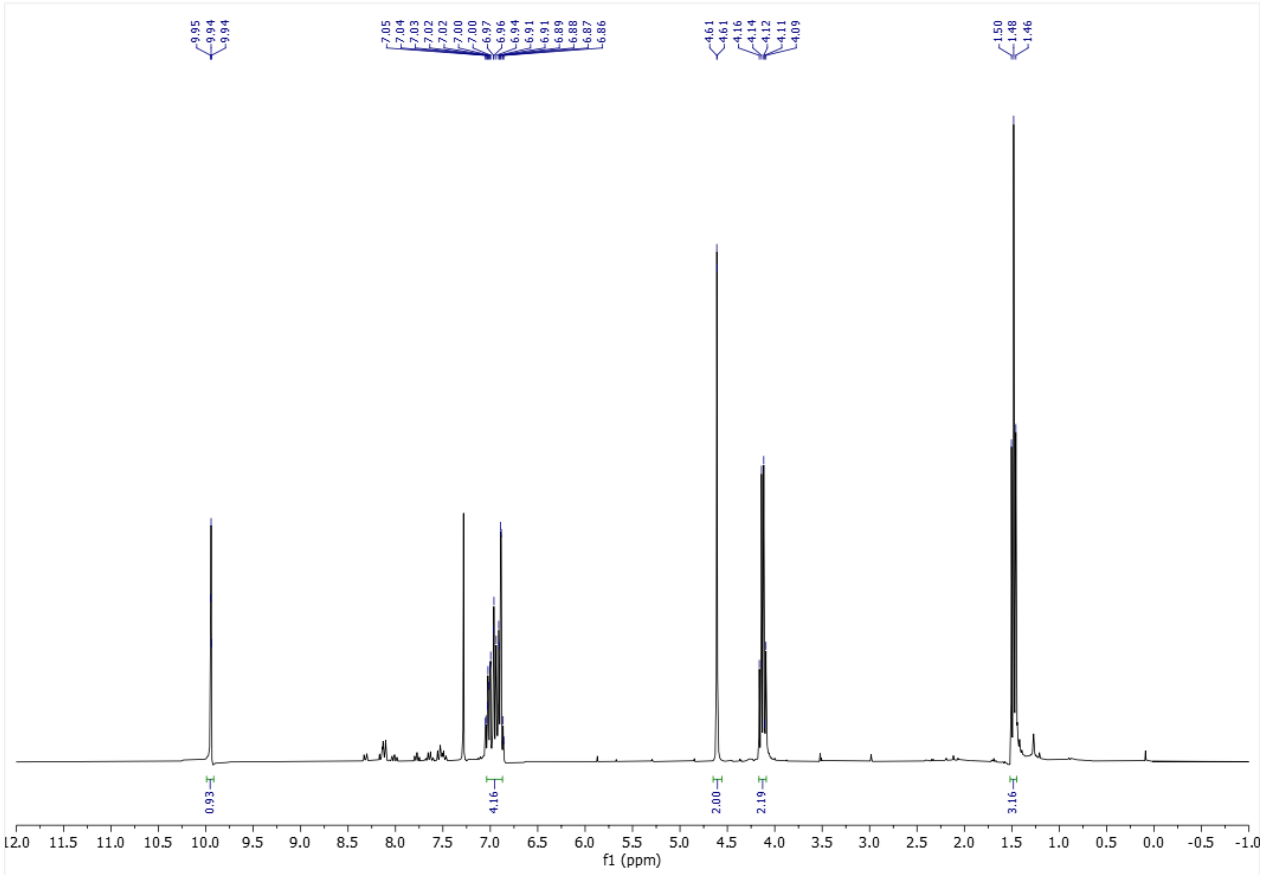

Figure S34. ^{1}H-NMR spectrum ($CDCl_3$) of compound **10**.

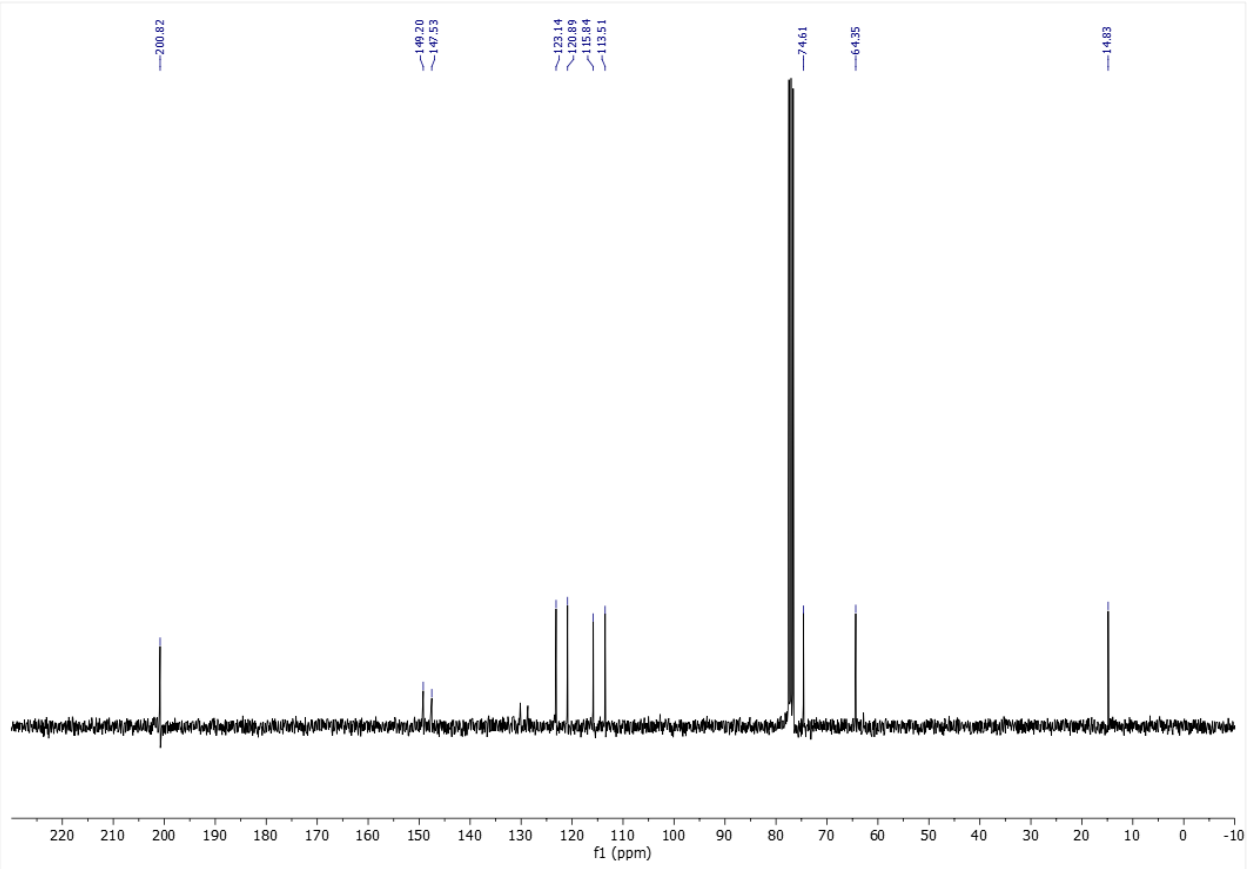

Figure S35. ^{13}C-NMR spectrum ($CDCl_3$) of compound **10**.

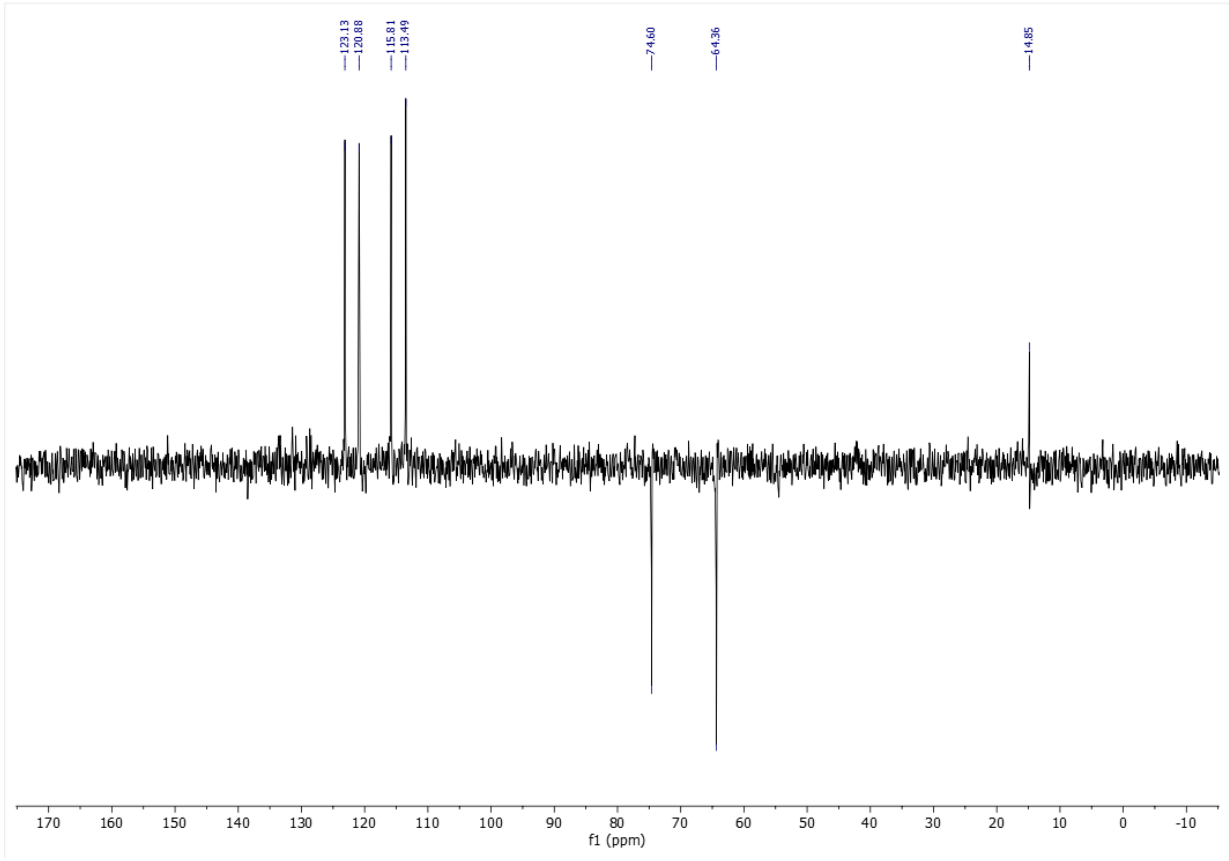

Figure S36. DEPT NMR spectrum ($CDCl_3$) of compound **10**.

2-(2-Ethoxyphenoxy)ethyl methanesulfonate (11)

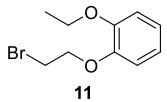

11

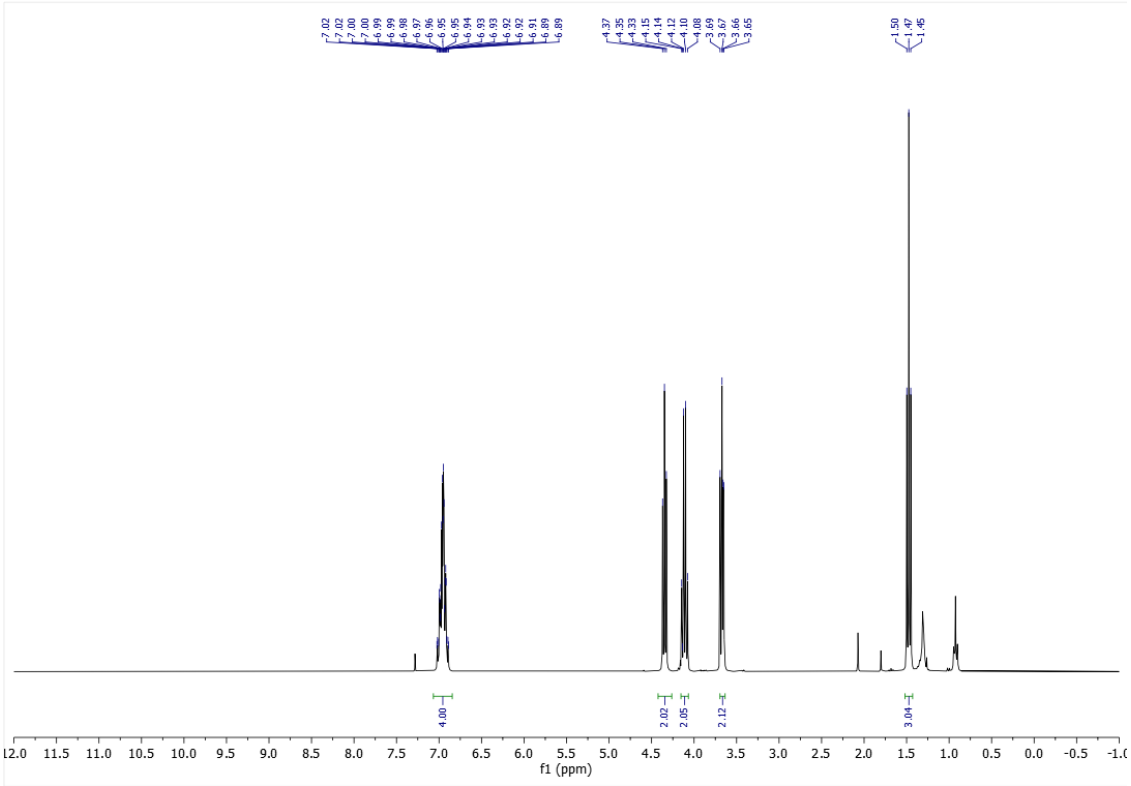

Figure S37. ^{1}H-NMR spectrum ($CDCl_3$) of compound **11**.

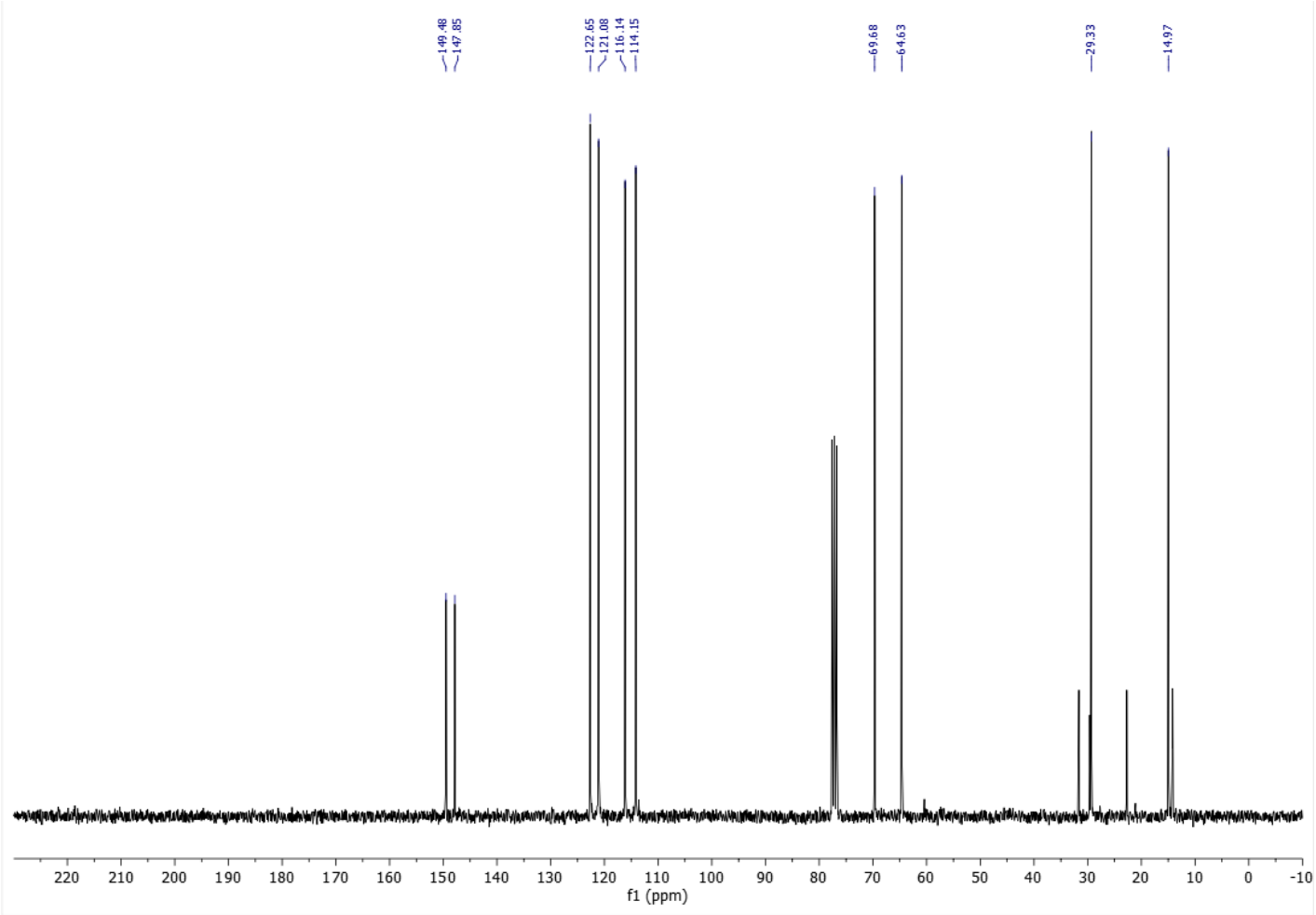

Figure S38. ^{13}C-NMR spectrum ($CDCl_3$) of compound **11**.

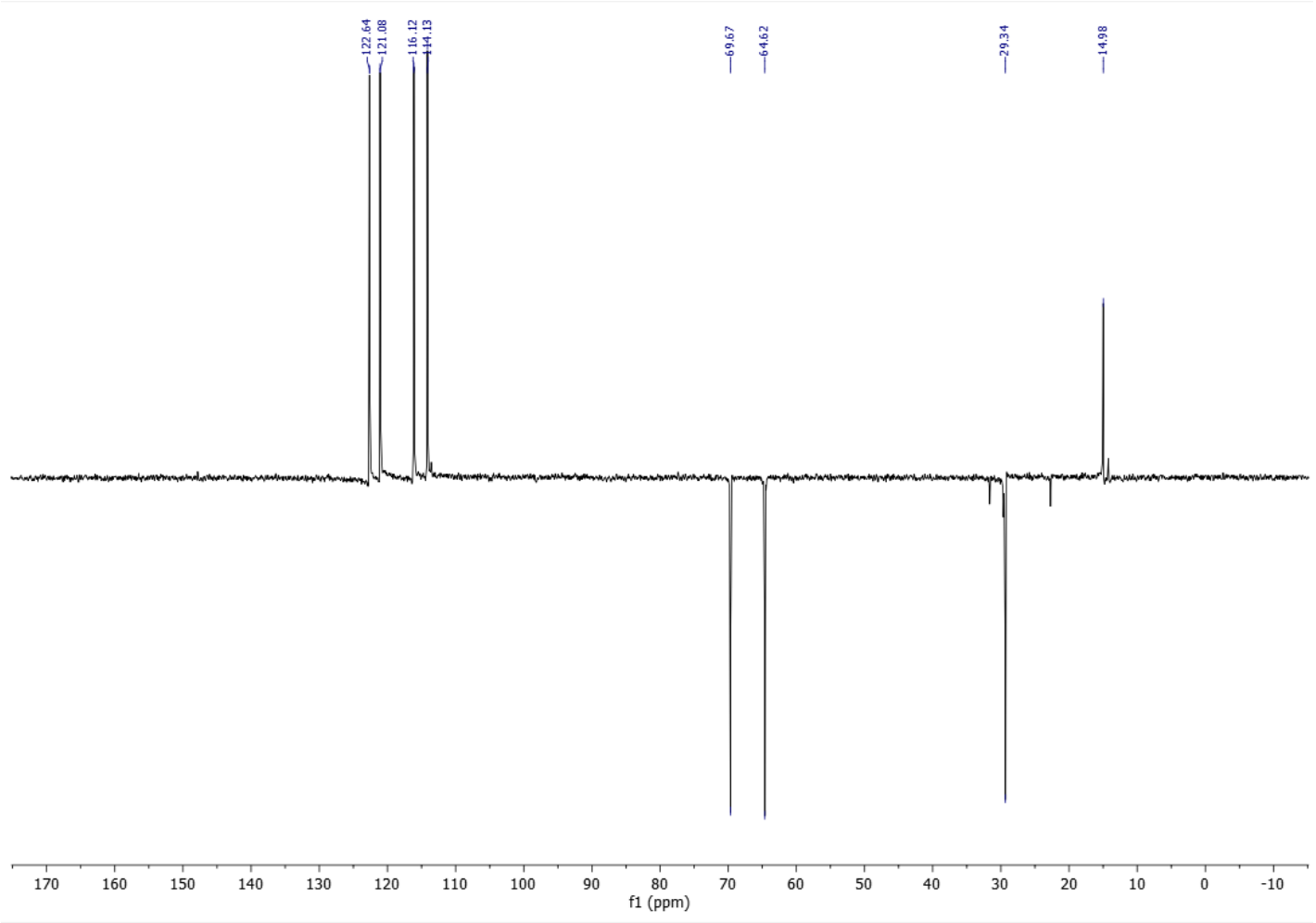

Figure S39. DEPT NMR spectrum ($CDCl_3$) of compound **11**.

1-(2-Bromoethoxy)-2-ethoxybenzene (12)

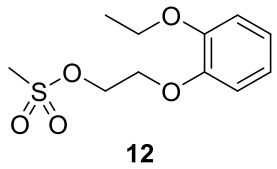

12

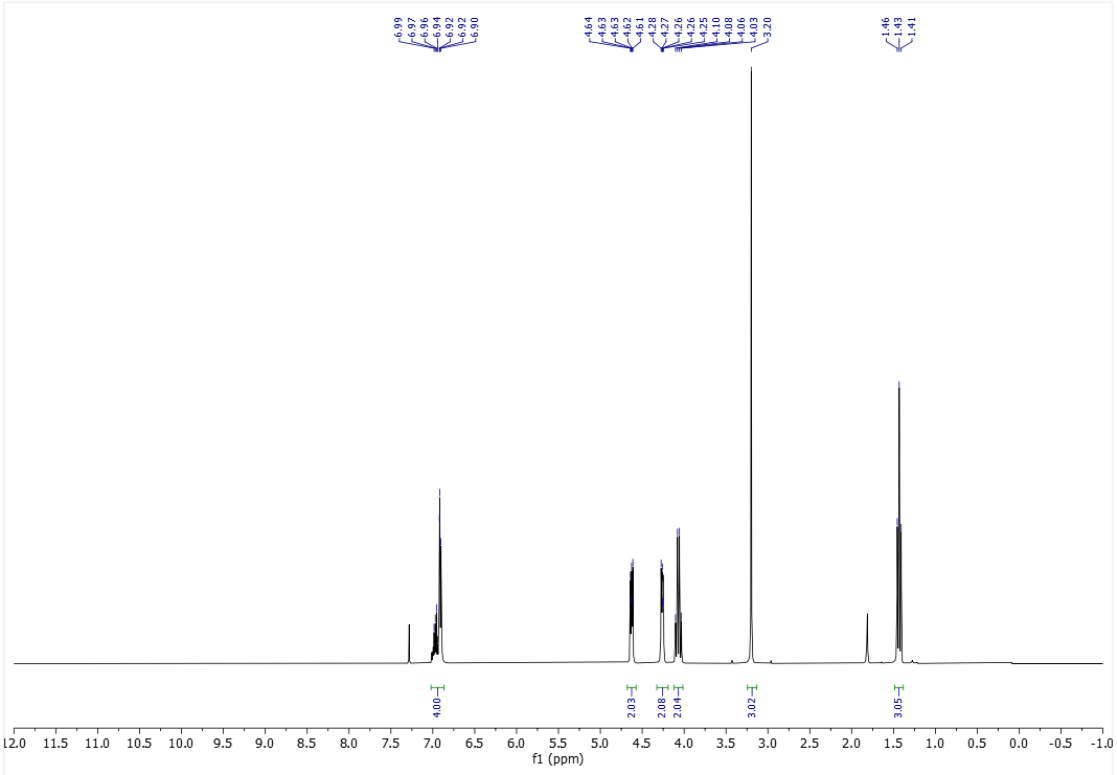

Figure S40. ^{1}H-NMR spectrum ($CDCl_3$) of compound **12**.

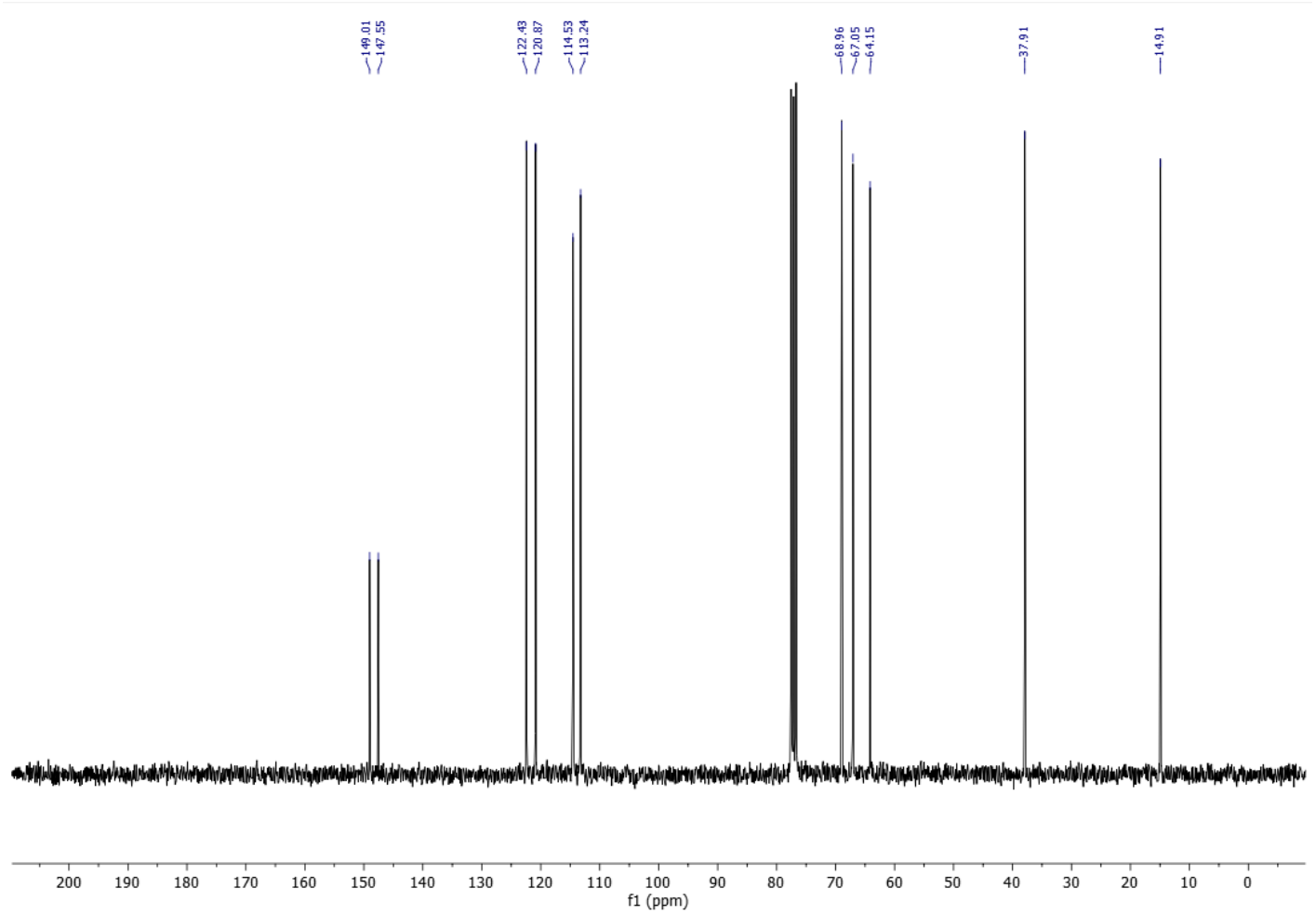

Figure S41. ^{13}C-NMR spectrum ($CDCl_3$) of compound **12**.

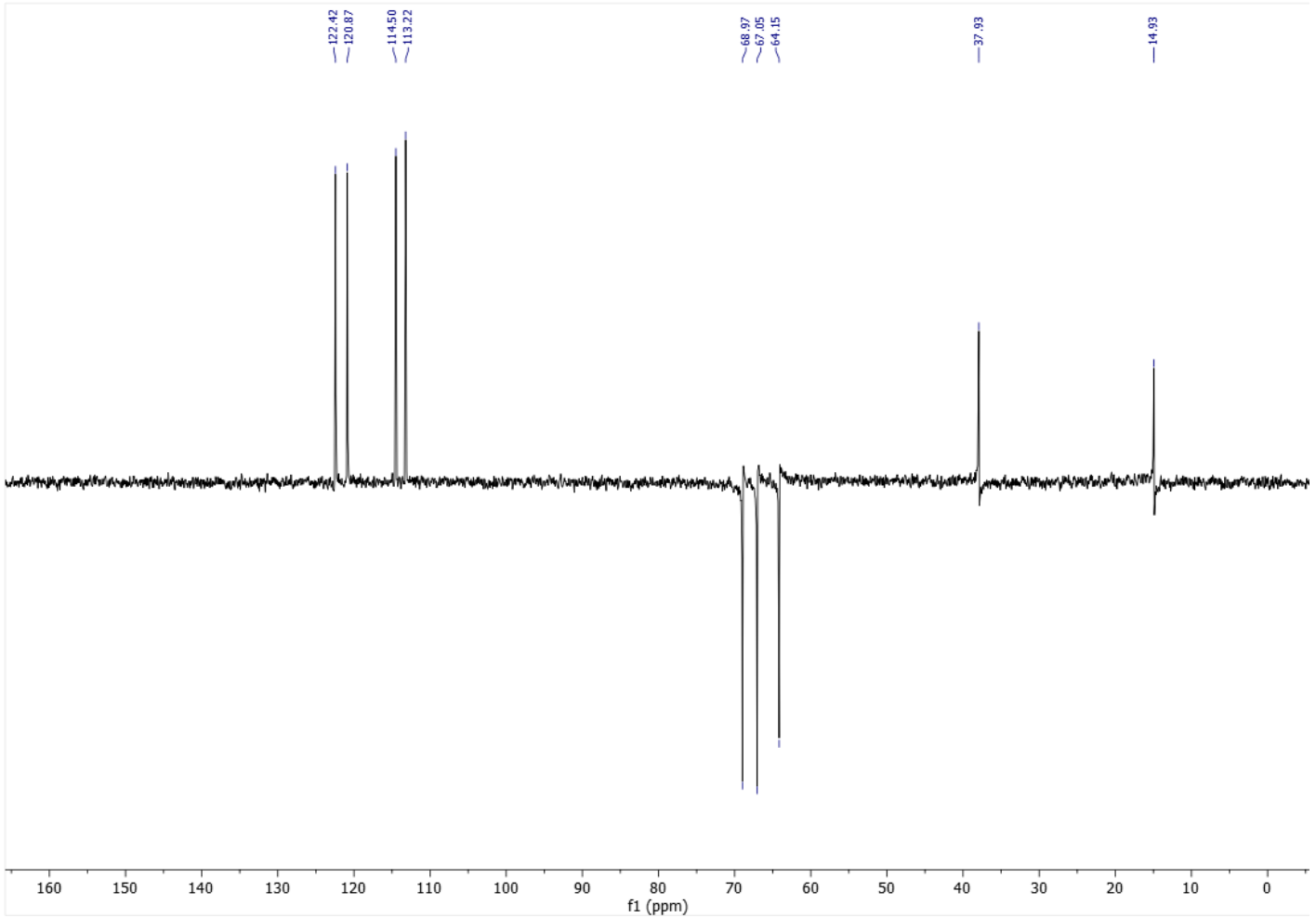

Figure S42. DEPT NMR spectrum ($CDCl_3$) of compound **12**

***N*-(tert-butyl)-2-methoxy-5-{2-[(2-(2-methoxyphenoxy)ethyl)amino]propyl}benzenesulfonamide (13)**

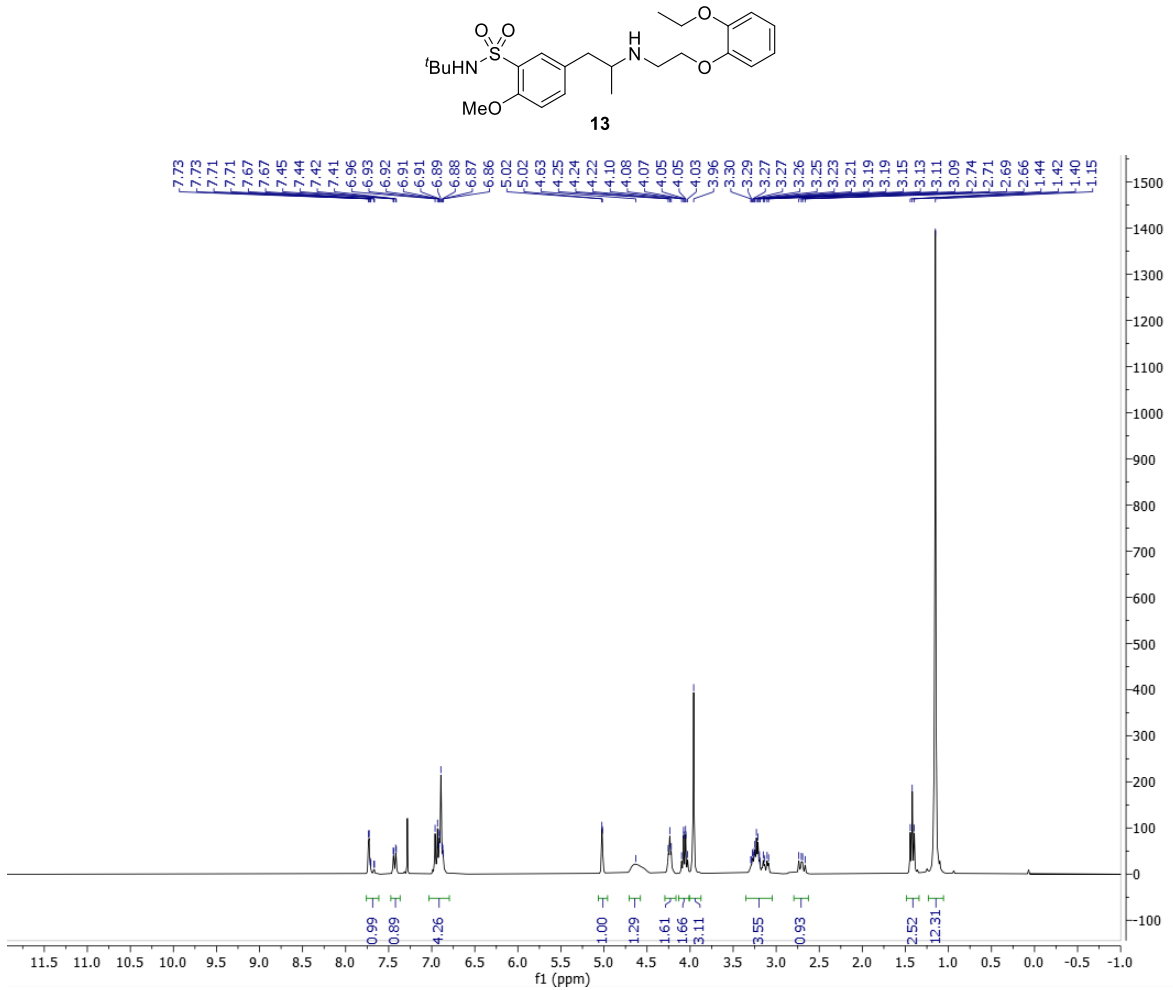

Figure S43. ^{1}H-NMR spectrum ($CDCl_3$) of compound **13**.

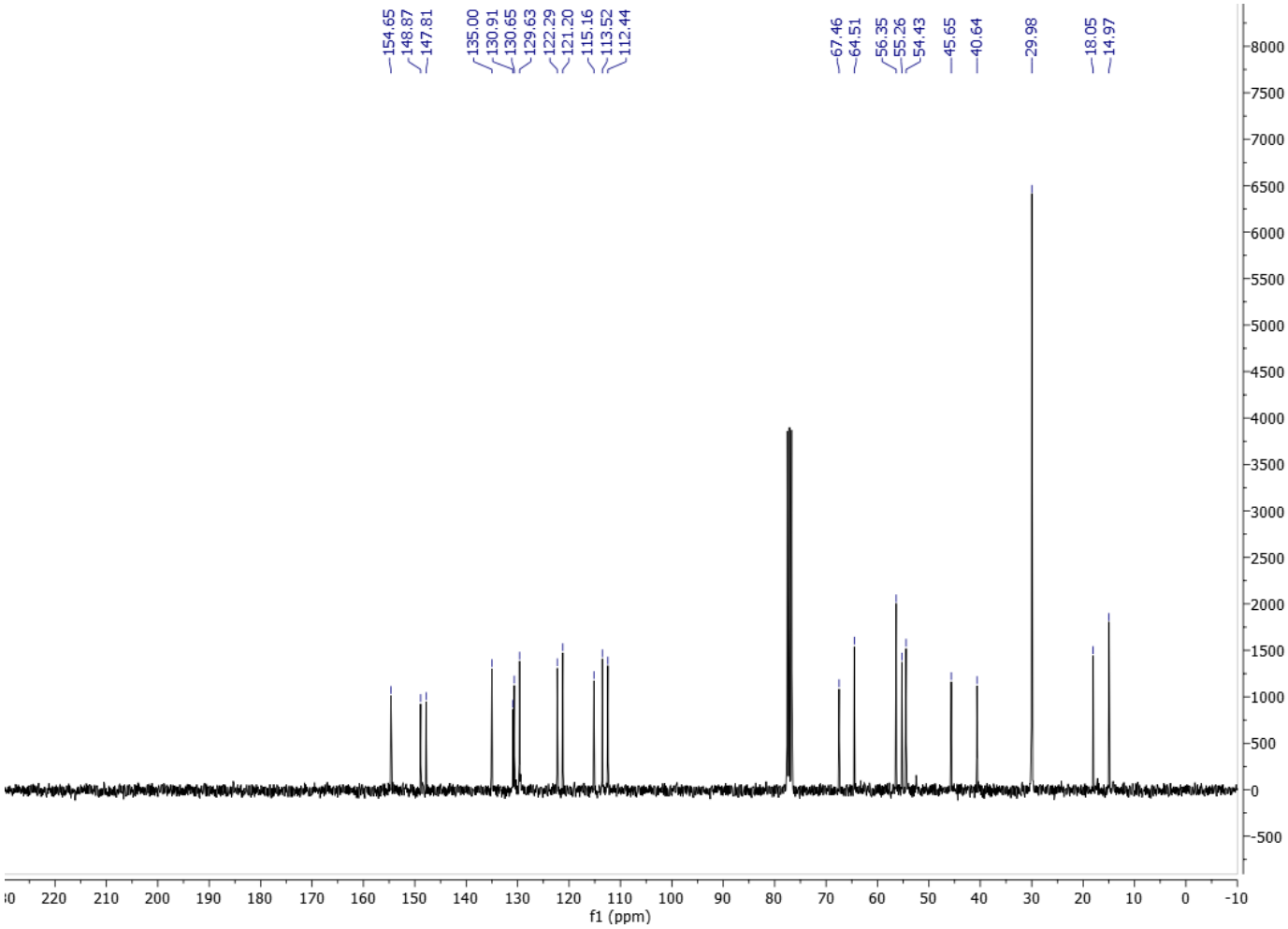

Figure S44. ^{13}C-NMR spectrum ($CDCl_3$) of compound **13**.

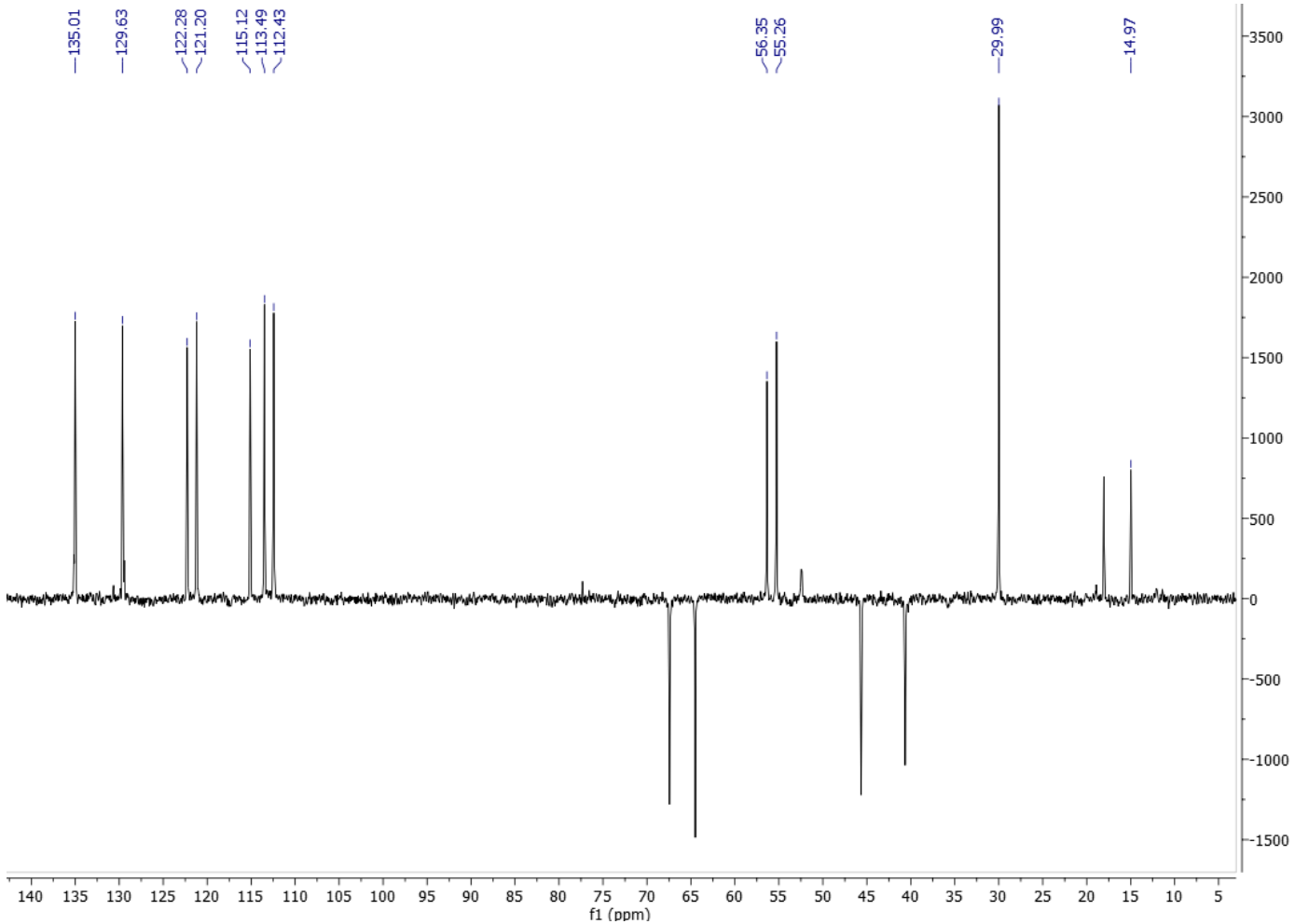

Figure S45. DEPT NMR spectrum ($CDCl_3$) of compound **13**.

5-{2-[(2-(2-Methoxyphenoxy)ethyl)amino]propyl}benzenesulfonamide (Tamsulosim, 1)

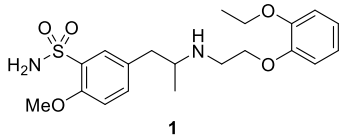

1

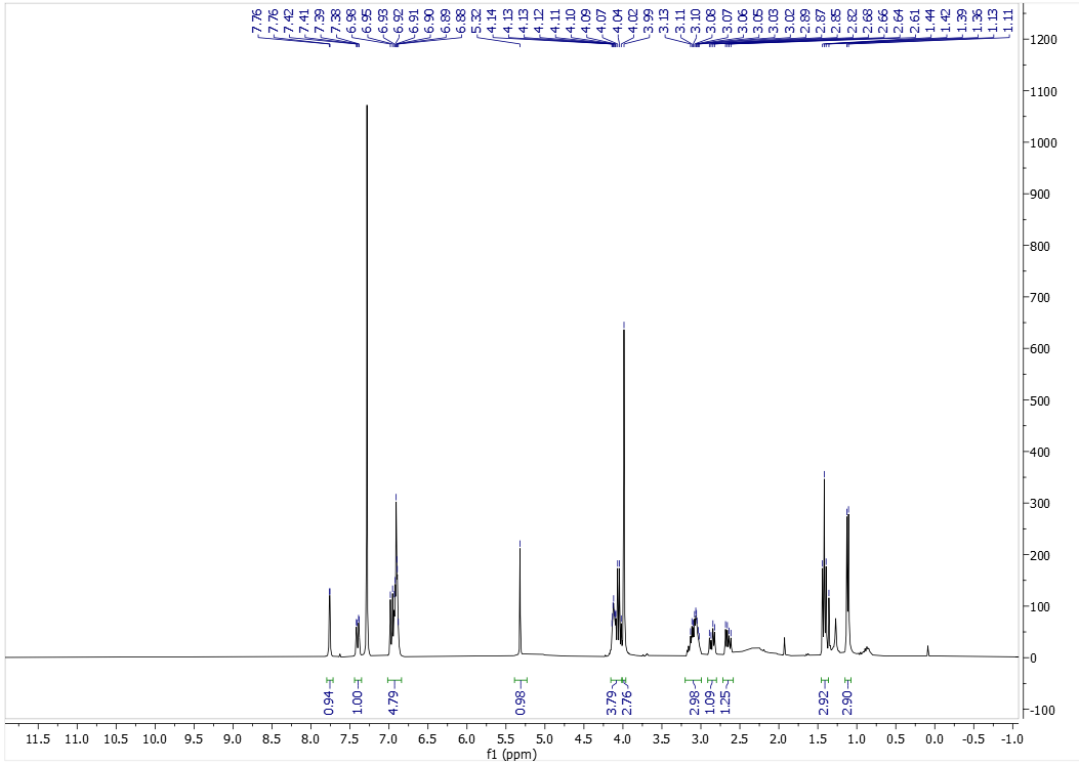

Figure S46. ^{1}H-NMR spectrum ($CDCl_3$) of compound **1**.

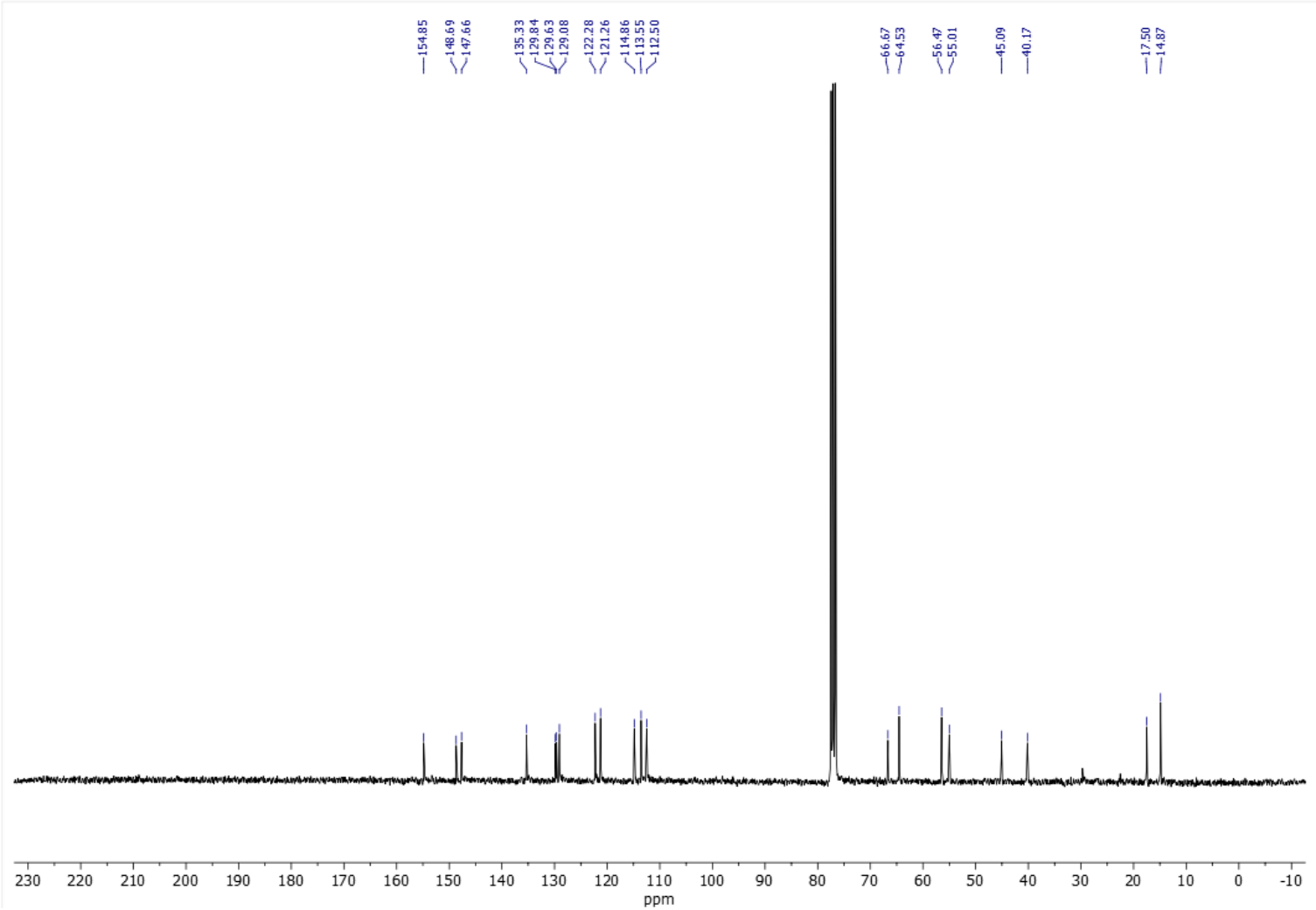

Figure S47. ^{13}C-NMR spectrum ($CDCl_3$) of compound **1**.

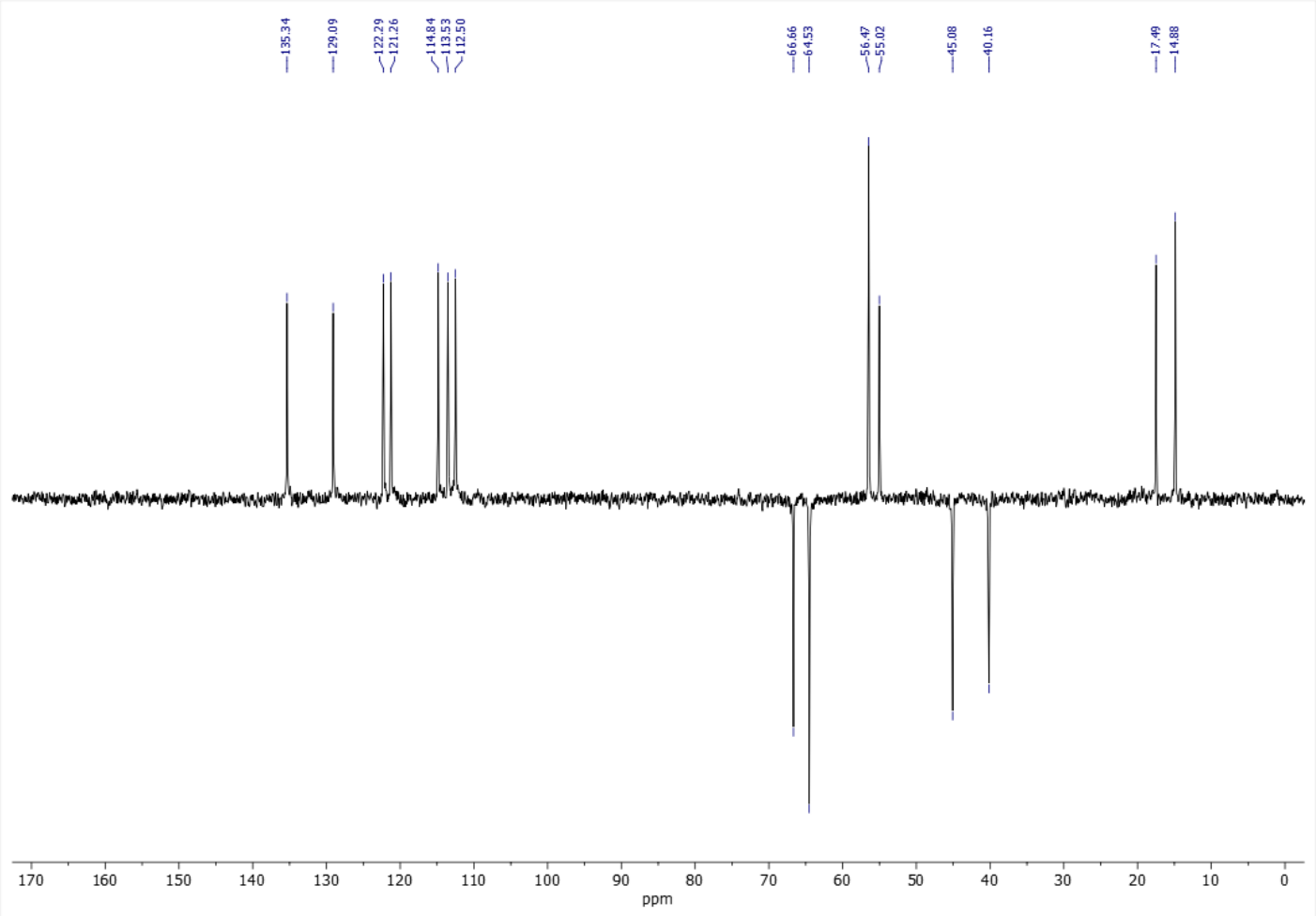

Figure S48. DEPT NMR spectrum ($CDCl_3$) of compound **1**.